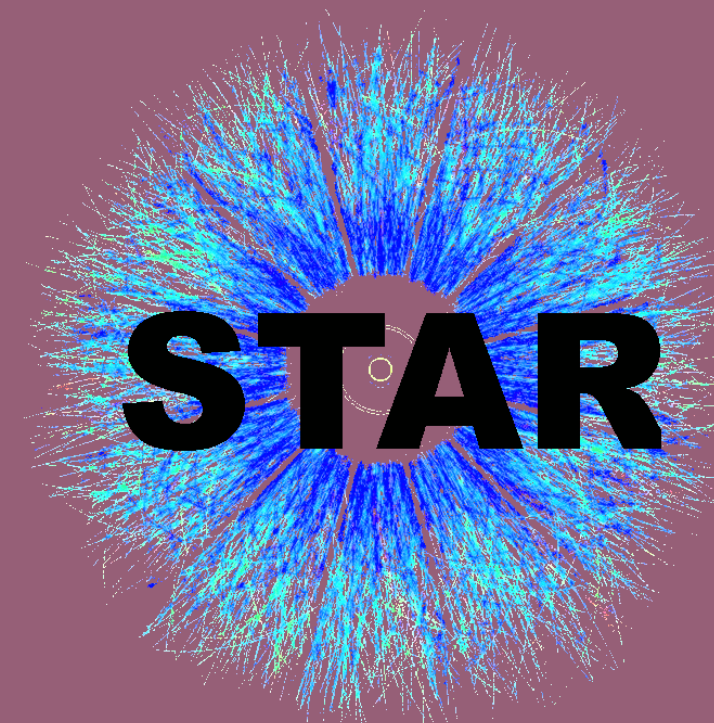




**Faculty
of Physics**

WARSAW UNIVERSITY OF TECHNOLOGY



Charged and neutral kaons femtoscopy measured by the STAR experiment

Diana Pawłowska (for the STAR Collaboration)

diana.pawlowska.dokt@pw.edu.pl

15th Workshop on Particle Correlations and Femtoscopy,
East Lansing, Michigan, USA

18 – 22 July, 2022

Partially funded by:



**U.S. DEPARTMENT OF
ENERGY**

Office of
Science



NATIONAL SCIENCE CENTRE
POLAND

**RESEARCH
UNIVERSITY**
EXCELLENCE INITIATIVE

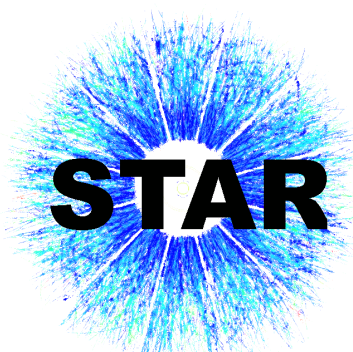
Femtoscopy - introduction

$$CF(\vec{q}) = \frac{P_{12}(\vec{p}_1, \vec{p}_2)}{P_1(\vec{p}_1)P_2(\vec{p}_2)} = \int d^3r S(\vec{q}, \vec{r}) |\Psi(\vec{q}, \vec{r})|^2 = \frac{A(\vec{q})}{B(\vec{q})}$$

\vec{p}_1, \vec{p}_2 - single particle momentum

$S(\vec{q}, \vec{r})$ – emission function
 $\Psi(\vec{q}, \vec{r})$ – pair wave function
 $\vec{q} = |\vec{p}_1 - \vec{p}_2|$ - relative momentum
 \vec{r} - relative distance between two particles

$A(\vec{q})$ - correlated
 $B(\vec{q})$ - uncorrelated



Femtoscopy - introduction

statistical	model	experiment
$CF(\vec{q}) = \frac{P_{12}(\vec{p}_1, \vec{p}_2)}{P_1(\vec{p}_1)P_2(\vec{p}_2)} = \int d^3r S(\vec{q}, \vec{r}) \Psi(\vec{q}, \vec{r}) ^2 = \frac{A(\vec{q})}{B(\vec{q})}$		

\vec{p}_1, \vec{p}_2 - single particle momentum

$S(\vec{q}, \vec{r})$ – emission function
 $\Psi(\vec{q}, \vec{r})$ – pair wave function
 $\vec{q} = |\vec{p}_1 - \vec{p}_2|$ - relative momentum
 \vec{r} - relative distance between two particles

Kaon correlation functions are sensitive to:

$K^\pm K^\pm$

$K_s^0 K_s^0$

$K_s^0 K^\pm$

Quantum Statistical effects (QS)

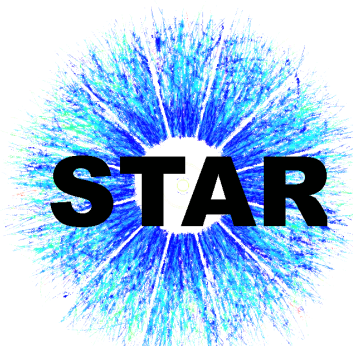
Final State Interaction (FSI)
- Coulomb interaction (COUL)

Quantum Statistical effects (QS)

Final State Interaction (FSI)
- strong interaction (SI)

Final State Interaction (FSI)

- strong interaction (SI)



Femtoscopy - introduction

$$CF(\vec{q}) = \frac{P_{12}(\vec{p}_1, \vec{p}_2)}{P_1(\vec{p}_1)P_2(\vec{p}_2)} = \int d^3r S(\vec{q}, \vec{r}) |\Psi(\vec{q}, \vec{r})|^2 = \frac{A(\vec{q})}{B(\vec{q})}$$

\vec{p}_1, \vec{p}_2 - single particle momentum

$S(\vec{q}, \vec{r})$ – emission function
 $\Psi(\vec{q}, \vec{r})$ – pair wave function

$\vec{q} = |\vec{p}_1 - \vec{p}_2|$ - relative momentum
 \vec{r} - relative distance between two particles

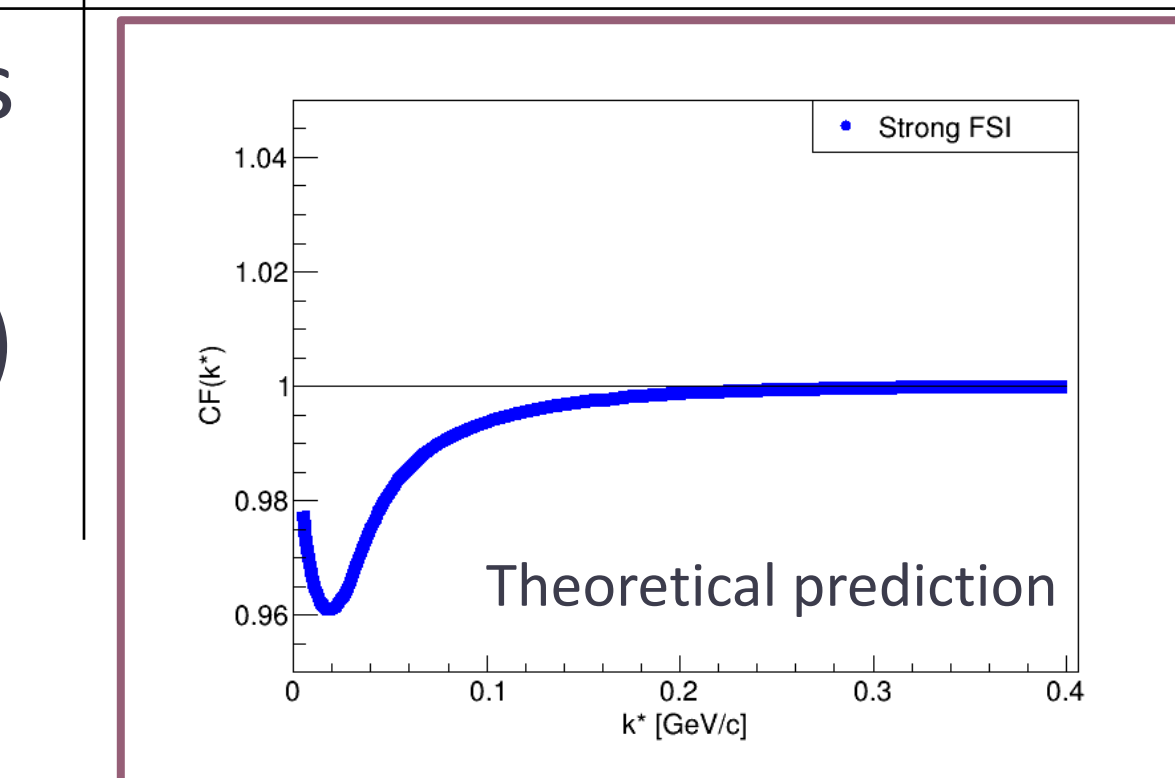
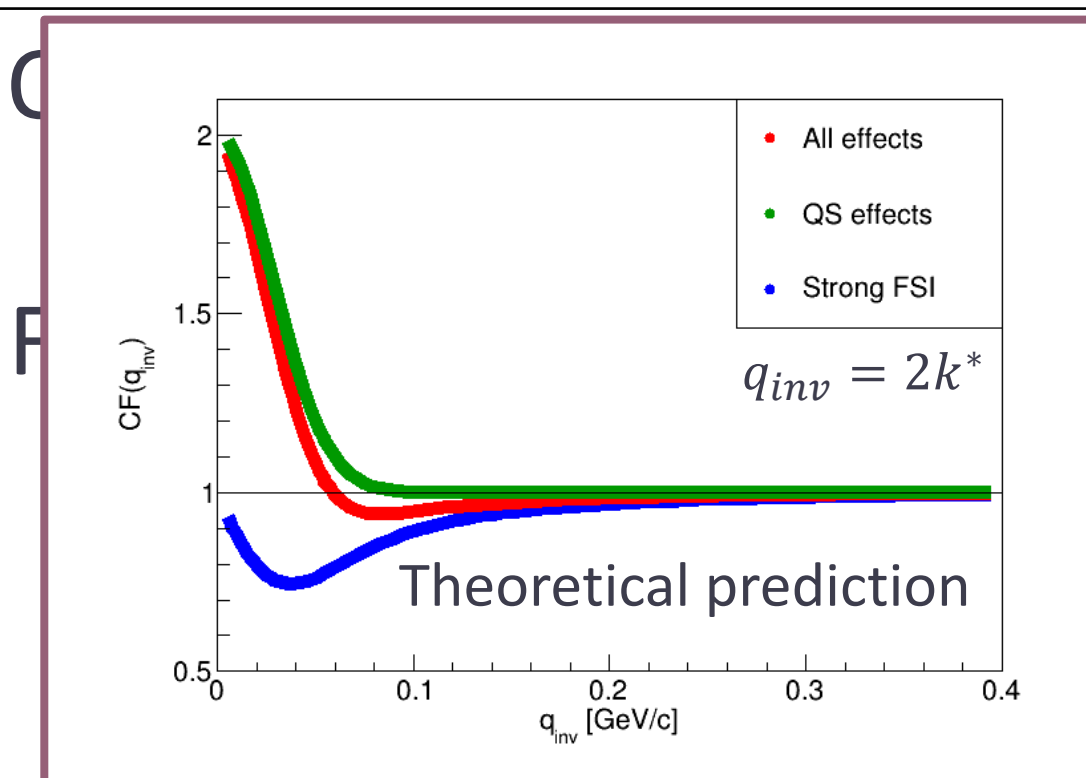
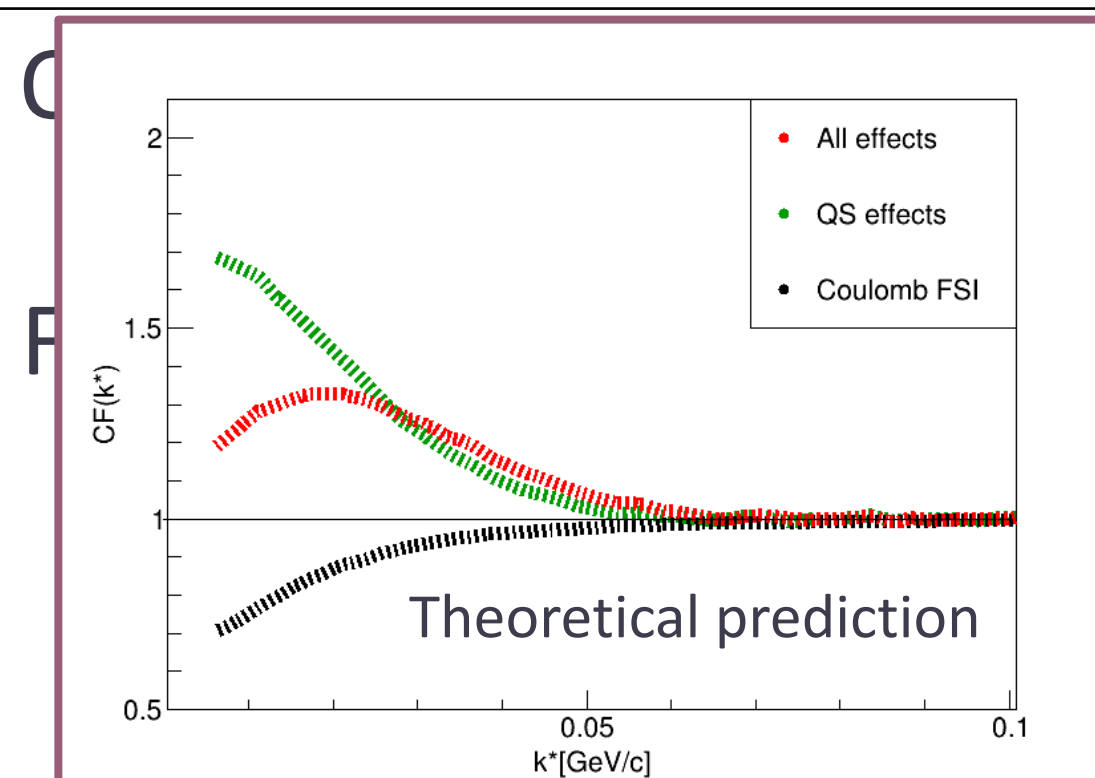
$A(\vec{q})$ - correlated
 $B(\vec{q})$ - uncorrelated

Kaon correlation functions are sensitive to:

$K^\pm K^\pm$

$K_s^0 K_s^0$

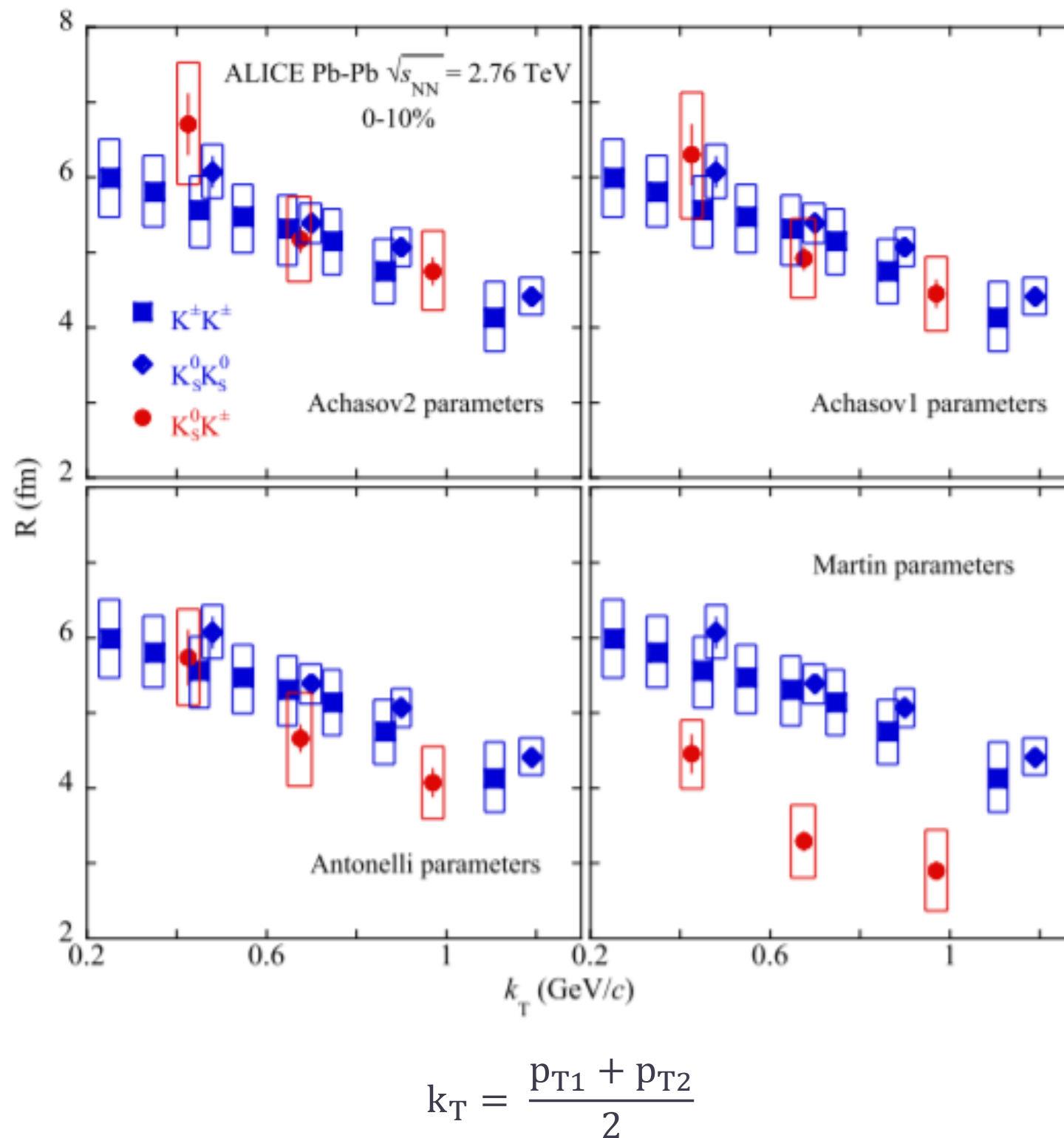
$K_s^0 K^\pm$



k^* - first particle momentum in PRF

Motivation

ALICE, Physics Letters B 774(2017) 64

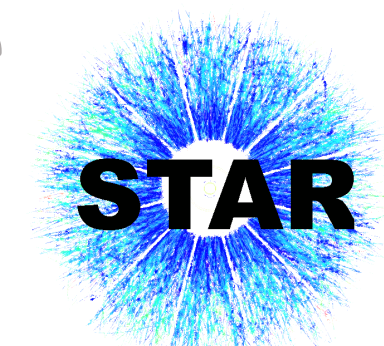


Kaons provide complementary information to pions:

- contain strange quarks (larger production of strange particles is one of the signatures of QGP)
- less affected by the feed-down from resonance decays
- smaller cross section on reaction with the hadronic matter

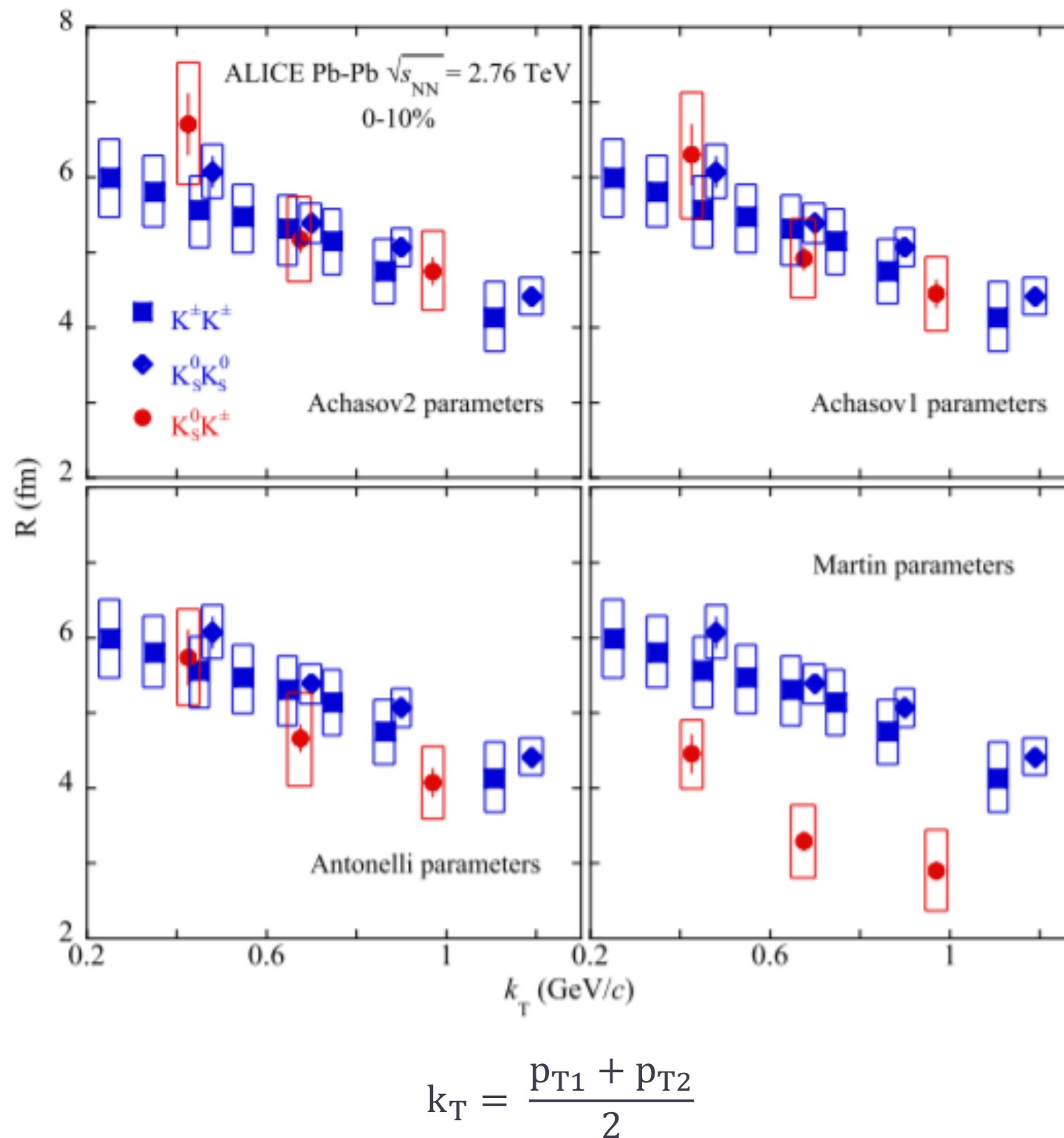
Very interesting:

- compare femtoscopic results for all possible kaon combination ($K^\pm K^\pm$, $K_S^0 K_S^0$, $K_S^0 K^\pm$)
- $K_S^0 K^\pm$ - a_0 could be a 4-quark state (a tetraquark)



Motivation

ALICE, Physics Letters B 774(2017) 64



Kaons can provide complementary information to pions:

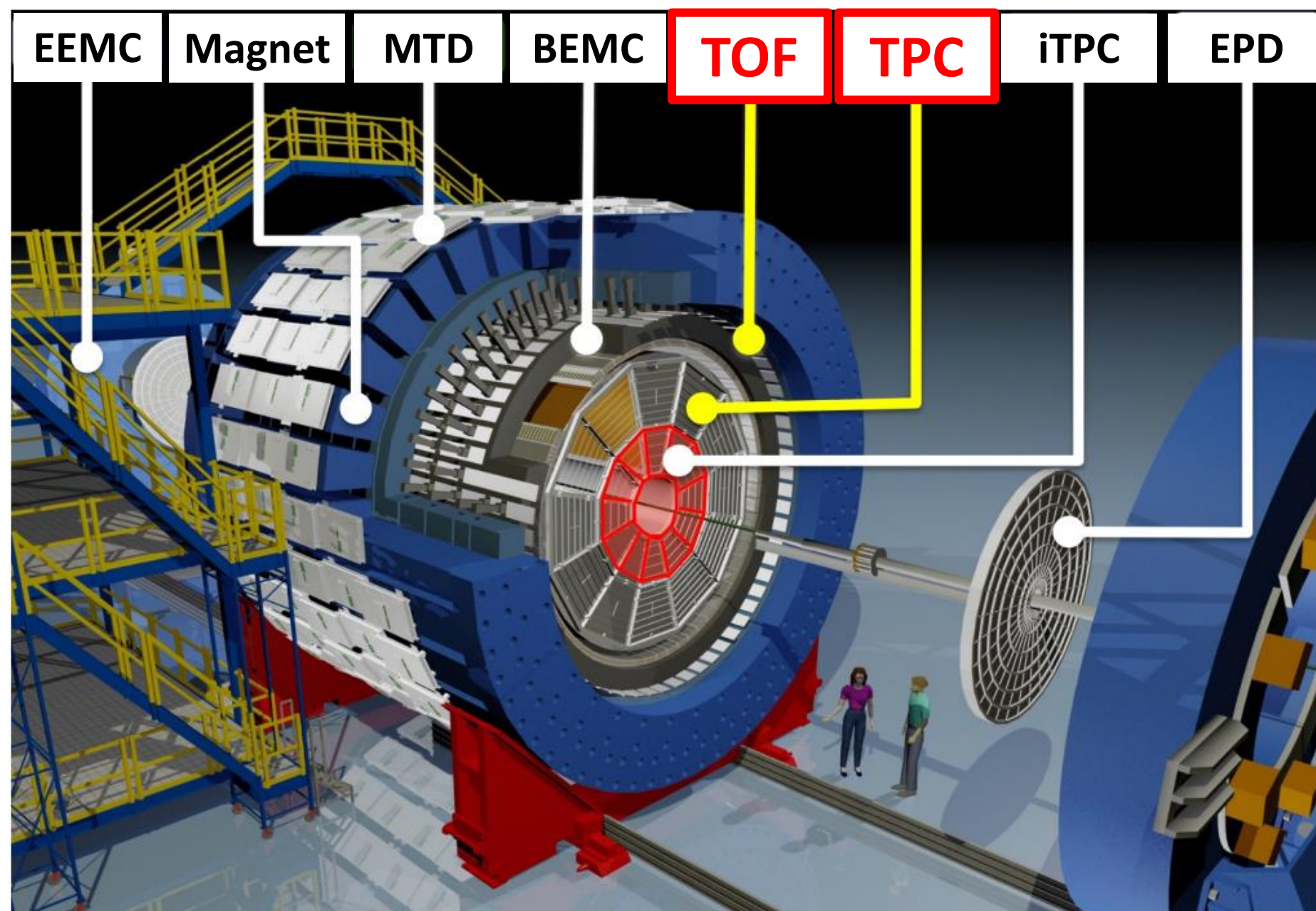
- contain strange quarks (larger production of strange particles is one of the signatures of QGP)
- less affected by the feed-down from resonance decays
- smaller cross section on reaction with the hadronic matter

Very interesting:

- compare femtoscopic results for all possible kaon combination ($K^{\pm}K^{\pm}$, $K_S^0K_S^0$, $K_S^0K^{\pm}$)
- $K_S^0K^{\pm}$ - a_0 could be a 4-quark state (a tetraquark)



The STAR experiment



- Excellent particle identification
- Large, uniform acceptance at mid-rapidity

Time Projection Chamber

PID: dE/dx

Tracking

$$0 < \phi < 2\pi, |\eta| < 1$$

Time-Of-Flight

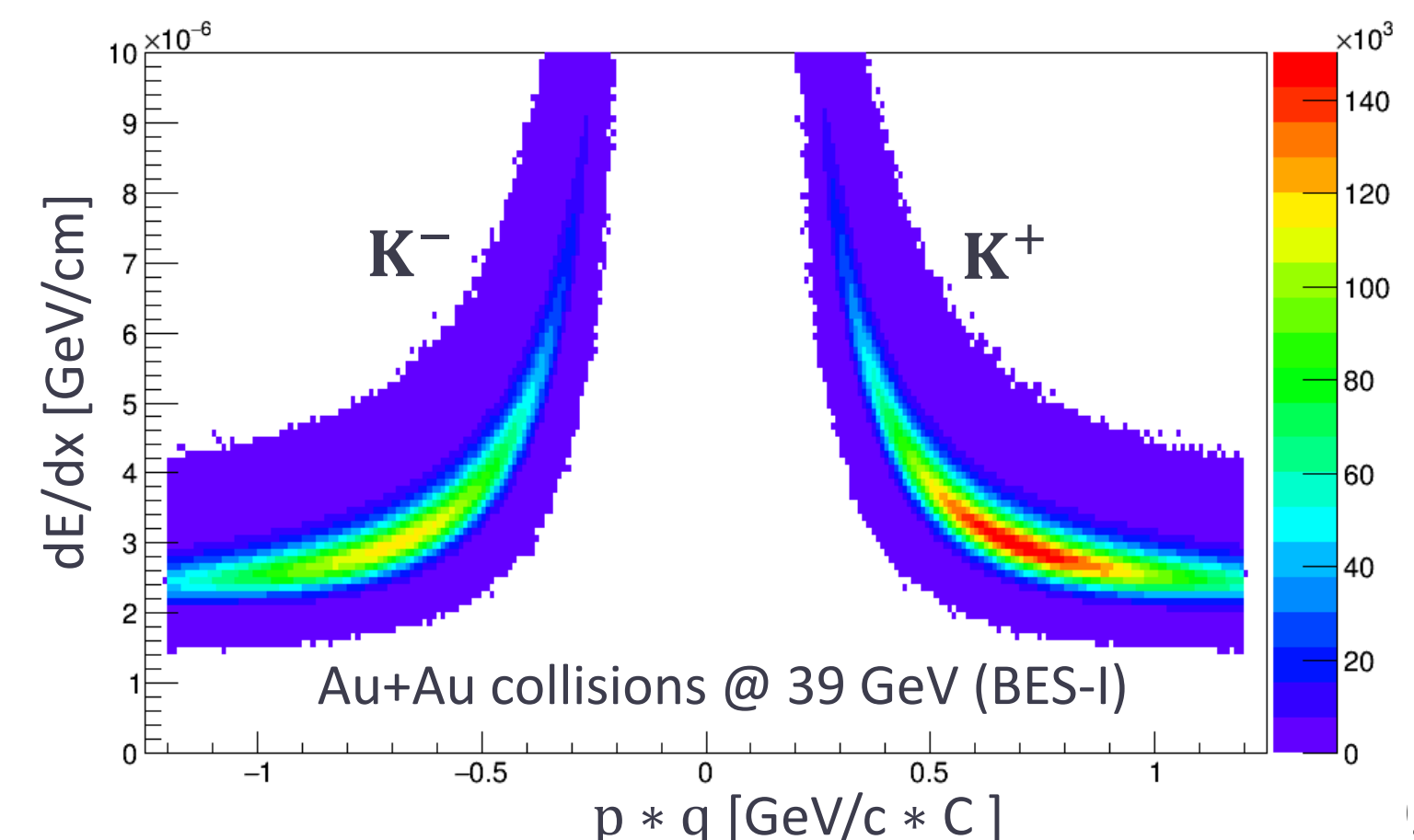
Time resolution < 80 ps

PID: m^2

Datasets

Energy $\sqrt{s_{NN}}$	Year	Mode	Statistics (M)
39 GeV	2010	Collider	~ 83
200 GeV	2010	Collider	~ 260

Au+Au collisions

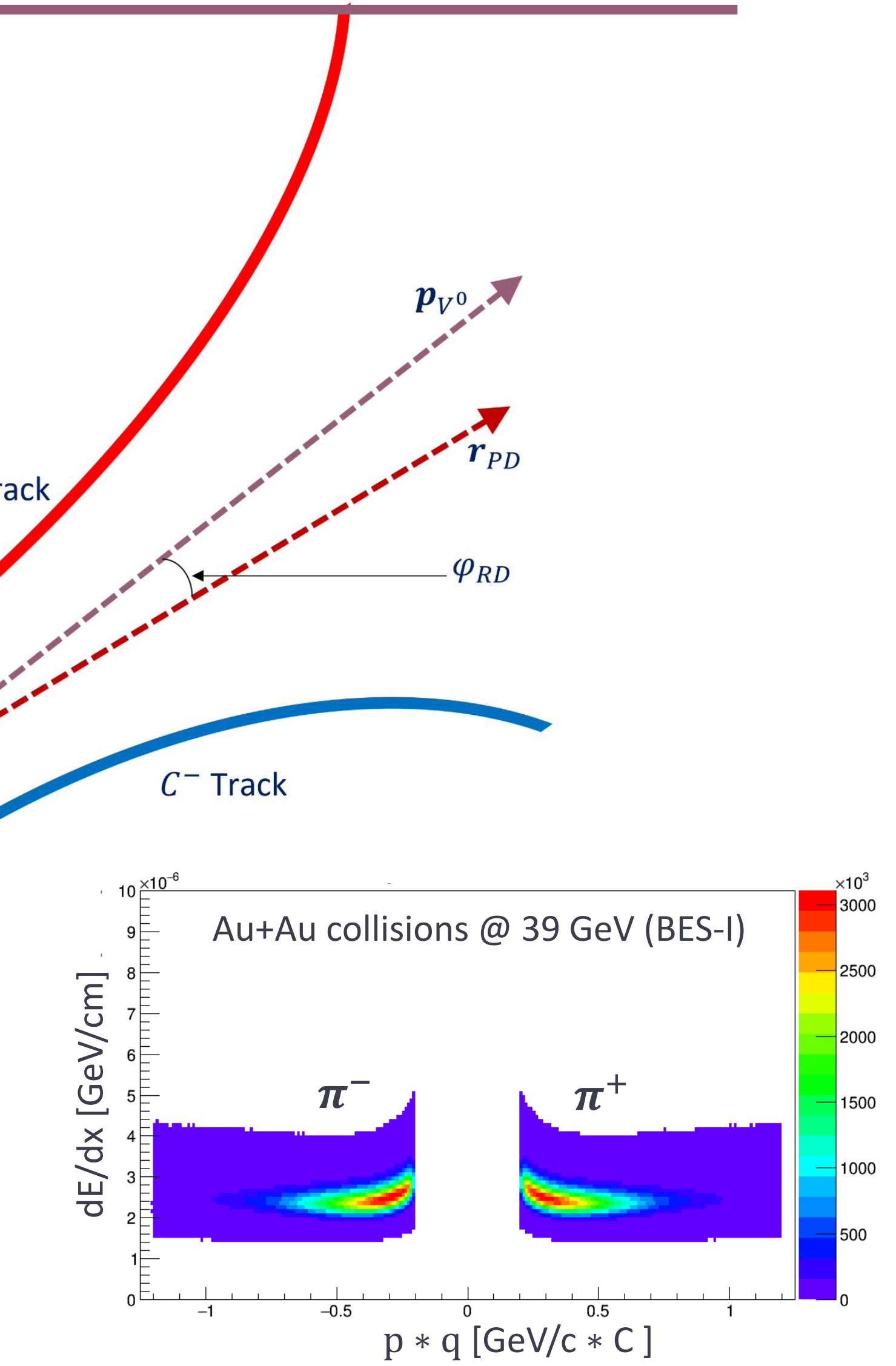
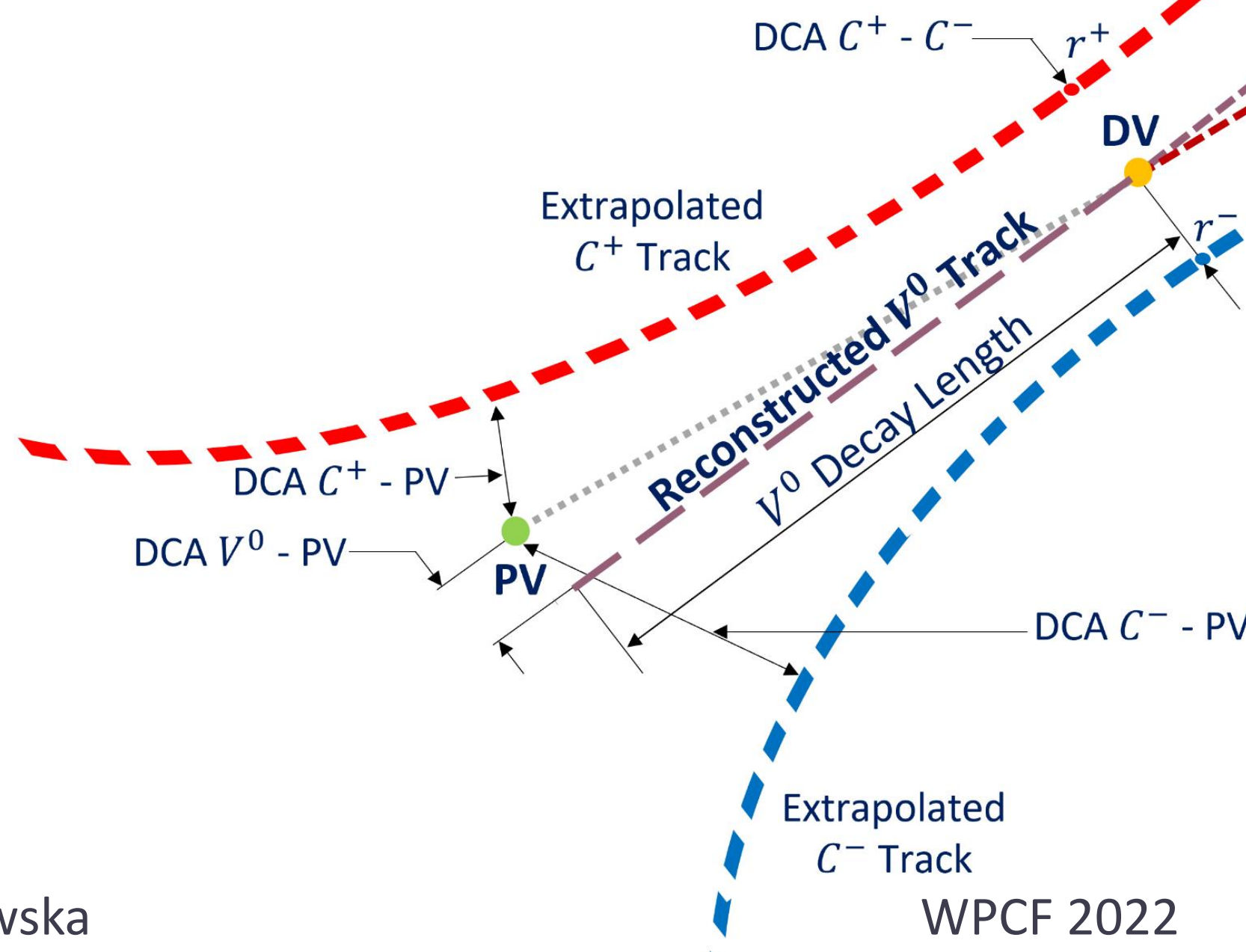


Neutral kaon reconstruction

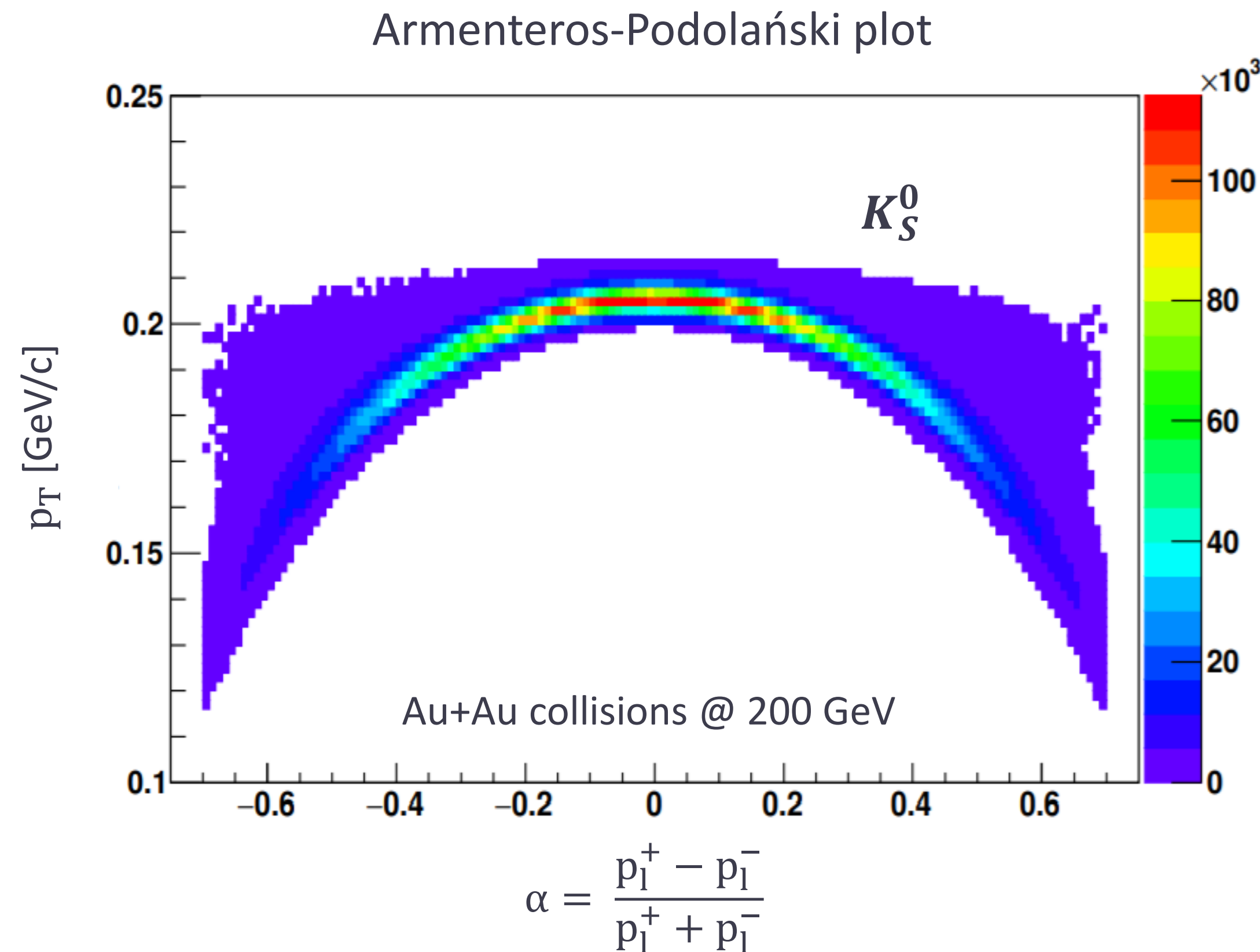
V^0 - neutral reconstructed particle
 C^\pm – positive/negative charged decay particle
 r^\pm – positive/negative charged decay particle position
PV – primary vertex
DV – decay vertex
DCA – distance of closest approach
 \mathbf{p}_{V^0} – V^0 reconstructed momentum vector
 \mathbf{r}_{PD} – vector from PV to DV
 φ_{RD} – angle between \mathbf{r}_{PD} and \mathbf{p}_{V^0}

$$K_S^0 \rightarrow \pi^+ \pi^- (69.20 \pm 0.05)\%$$

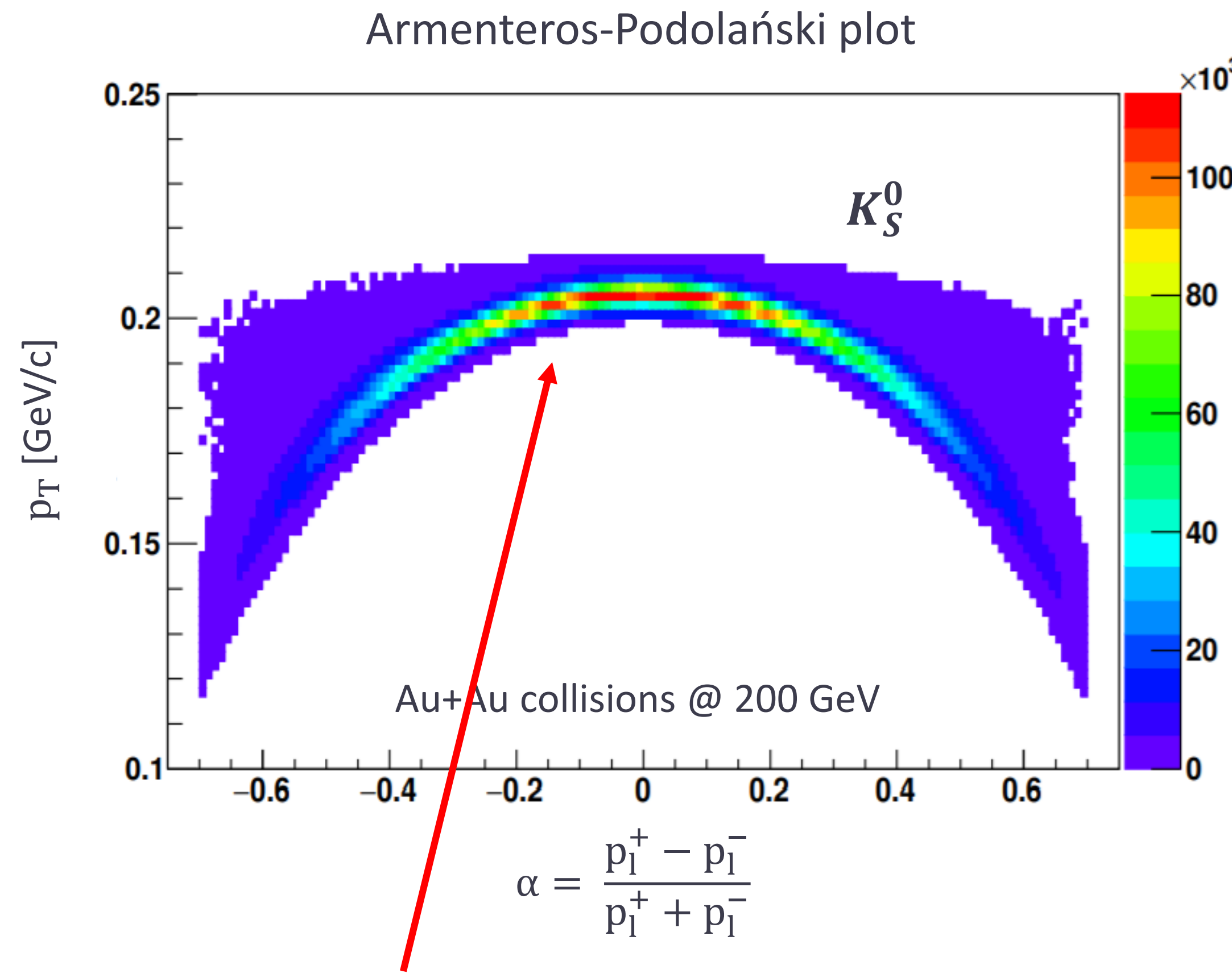
$$K_S^0 \rightarrow \pi^0 \pi^0 (30.69 \pm 0.05)\%$$



Neutral kaon reconstruction



Neutral kaon reconstruction



Decay products of the neutral kaon have the same mass and therefore their momenta are distributed symmetrically on average

Parametrization - $K_S^0 K_S^0$

Gaussian density distribution (includes only QS effects): $CF(q_{inv}) = 1 + \lambda e^{[-R_{inv}^2 q_{inv}^2]}$

λ - the correlation strength, R_{inv} - the size of the particle-emitting source.

Lednicky & Lyuboshitz model includes strong FSI: [Sov.J.Nucl.Phys. 35, 770 (1982)]

$$CF(q_{inv}) = 1 + \lambda \left(e^{[-R_{inv}^2 q_{inv}^2]} + \frac{1}{2} \left[\left| \frac{f(k^*)}{R_{inv}} \right|^2 + \frac{4\Re f(k^*)}{\sqrt{\pi} R_{inv}} F_1(q_{inv} R_{inv}) - \frac{2\Im f(k^*)}{\sqrt{\pi} R_{inv}} F_2(q_{inv} R_{inv}) \right] \right)$$



Parametrization - $K_S^0 K_S^0$

Gaussian density distribution (includes only QS effects): $CF(q_{inv}) = 1 + \lambda e^{[-R_{inv}^2 q_{inv}^2]}$

λ - the correlation strength, R_{inv} - the size of the particle-emitting source.

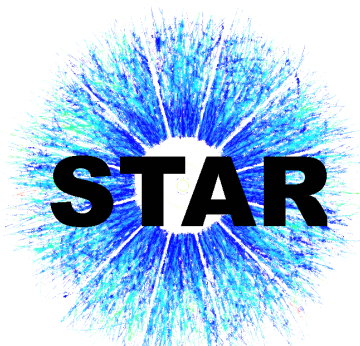
Lednicky & Lyuboshitz model includes strong FSI: [Sov.J.Nucl.Phys. 35, 770 (1982)]

$$CF(q_{inv}) = 1 + \lambda \left(e^{[-R_{inv}^2 q_{inv}^2]} + \frac{1}{2} \left[\left| \frac{f(k^*)}{R_{inv}} \right|^2 + \frac{4\Re f(k^*)}{\sqrt{\pi} R_{inv}} F_1(q_{inv} R_{inv}) - \frac{2\Im f(k^*)}{\sqrt{\pi} R_{inv}} F_2(q_{inv} R_{inv}) \right] \right)$$

QS effect **strong FSI through the $f_0(980)$ and $a_0(980)$ resonances**

$$F_1(z) = \int_0^z dx \frac{e^{x^2} - x^2}{z}, \quad F_2(z) = \frac{1 - e^{x^2}}{z}$$

$$f(k^*) = \frac{1}{2} [f_0(k^*) + f_1(k^*)], \quad f_I(k^*) = \frac{\gamma_r}{m_r - s - i\gamma_r k^* - i\gamma'_r k'_r}, \quad s = 4(m_K^2 + k^{*2})$$



Parametrization - $K_S^0 K_S^0$

Gaussian density distribution (includes only QS effects): $CF(q_{inv}) = 1 + \lambda e^{[-R_{inv}^2 q_{inv}^2]}$

λ - the correlation strength, R_{inv} - the size of the particle-emitting source.

Lednicky & Lyuboshitz model includes strong FSI: [Sov.J.Nucl.Phys. 35, 770 (1982)]

$$CF(q_{inv}) = 1 + \lambda \left(e^{[-R_{inv}^2 q_{inv}^2]} + \frac{1}{2} \left[\left| \frac{f(k^*)}{R_{inv}} \right|^2 + \frac{4\Re f(k^*)}{\sqrt{\pi} R_{inv}} F_1(q_{inv} R_{inv}) - \frac{2\Im f(k^*)}{\sqrt{\pi} R_{inv}} F_2(q_{inv} R_{inv}) \right] \right)$$

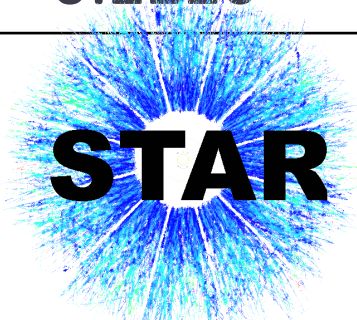
QS effect **strong FSI through the $f_0(980)$ and $a_0(980)$ resonances**

$$F_1(z) = \int_0^z dx \frac{e^{x^2} - x^2}{z}, \quad F_2(z) = \frac{1 - e^{x^2}}{z}$$

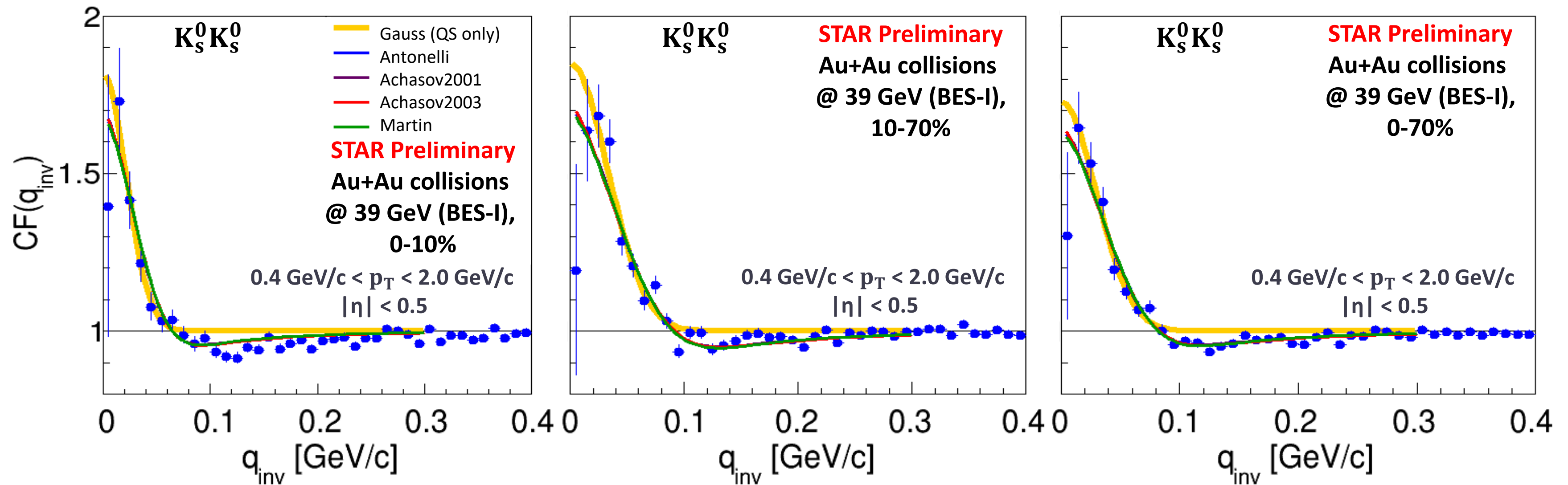
$$f(k^*) = \frac{1}{2} [f_0(k^*) + f_1(k^*)], \quad f_I(k^*) = \frac{\gamma_r}{m_r - s - i\gamma_r k^* - i\gamma'_r k'_r}, \quad s = 4(m_K^2 + k^{*2})$$

	$m_{f_0} \left[\frac{GeV}{c^2} \right]$	$\gamma_{f_0 K\bar{K}}$	$\gamma_{f_0 \pi\pi}$	$m_{a_0} \left[\frac{GeV}{c^2} \right]$	$\gamma_{a_0 K\bar{K}}$	$\gamma_{a_0 \pi\pi}$
Antonelli [1]	0.973	2.763	0.5283	0.985	0.4038	0.3711
Achasov2001 [2]	0.996	1.305	0.2684	0.992	0.5555	0.4401
Achasov2003 [3]	0.996	1.305	0.2684	1.003	0.8365	0.4580
Martin [4]	0.978	0.792	0.1990	0.974	0.3330	0.2220

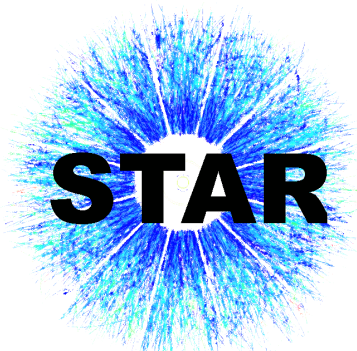
[1] eConf C020620, THAT06 (2002), [2] Phys. Rev. D 63, 094007 (2001)
 [3] Phys. Rev. D 68, 014006 (2003), [4] Nucl. Phys. B 121, 514–530 (1977)



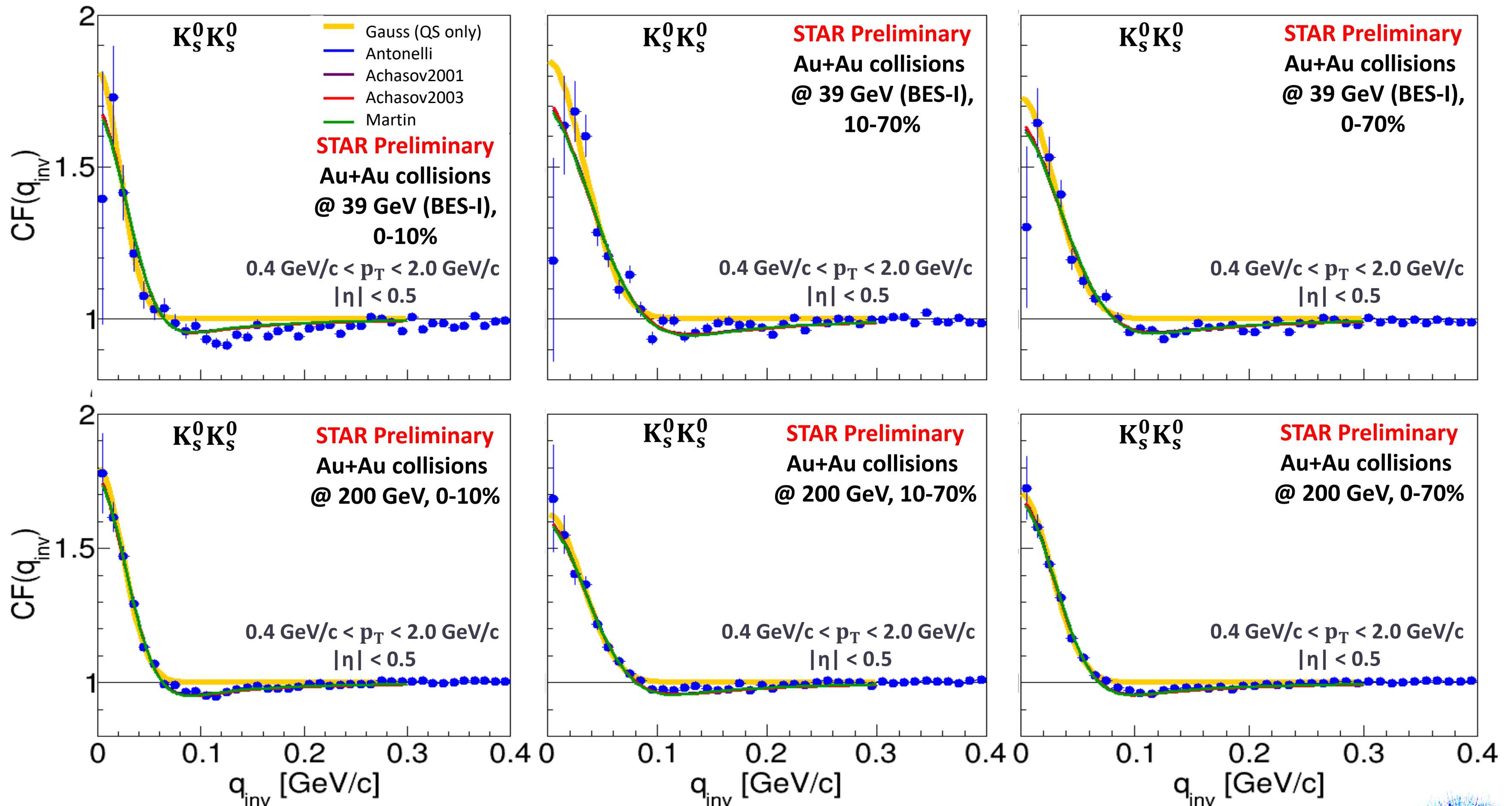
$K_s^0 K_s^0$ femtoscopy at 39 GeV & 200 GeV



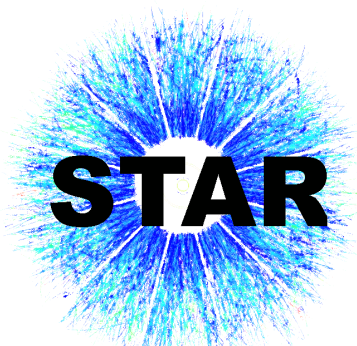
$$q_{\text{inv}} = \sqrt{(\vec{p}_1 - \vec{p}_2)^2 - (E_1 - E_2)^2}$$



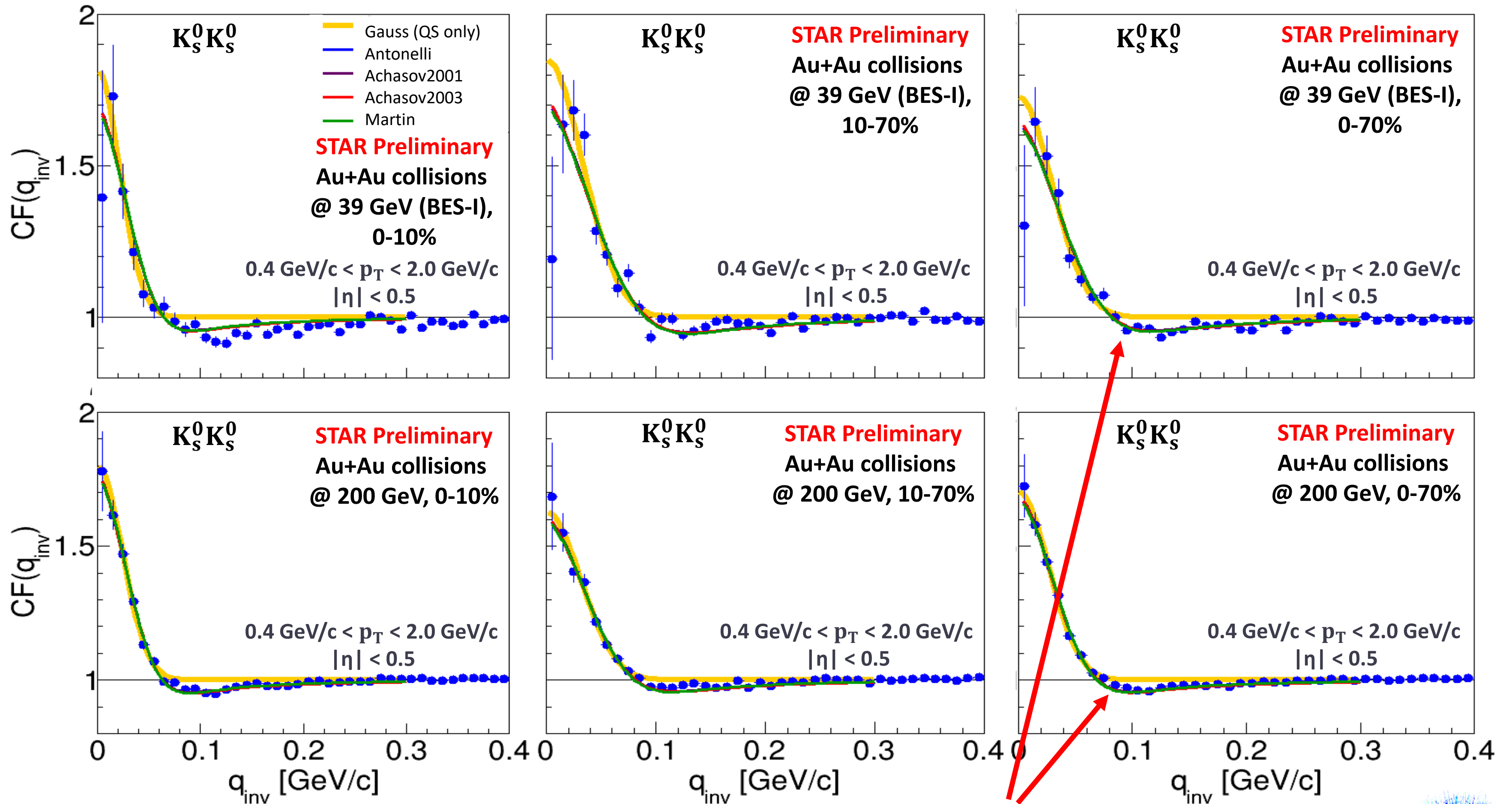
$K_s^0 K_s^0$ femtoscopy at 39 GeV & 200 GeV



$$q_{\text{inv}} = \sqrt{(\vec{p}_1 - \vec{p}_2)^2 - (E_1 - E_2)^2}$$



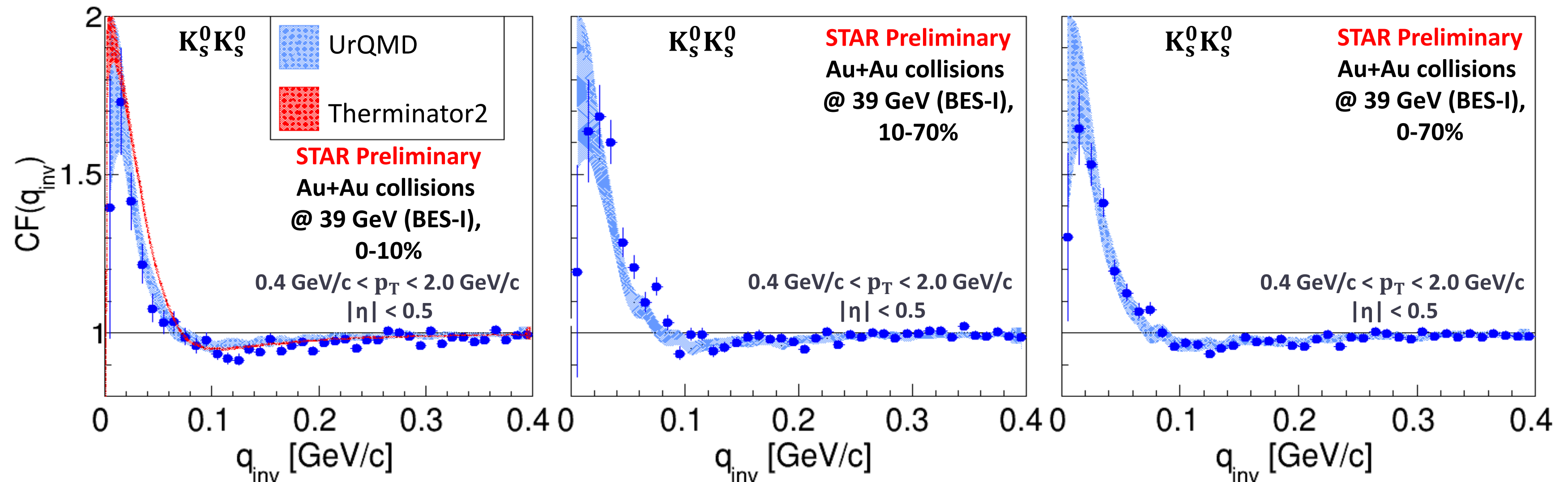
$K_s^0 K_s^0$ femtoscopy at 39 GeV & 200 GeV



**FSI is needed to reproduce
the dip structure**

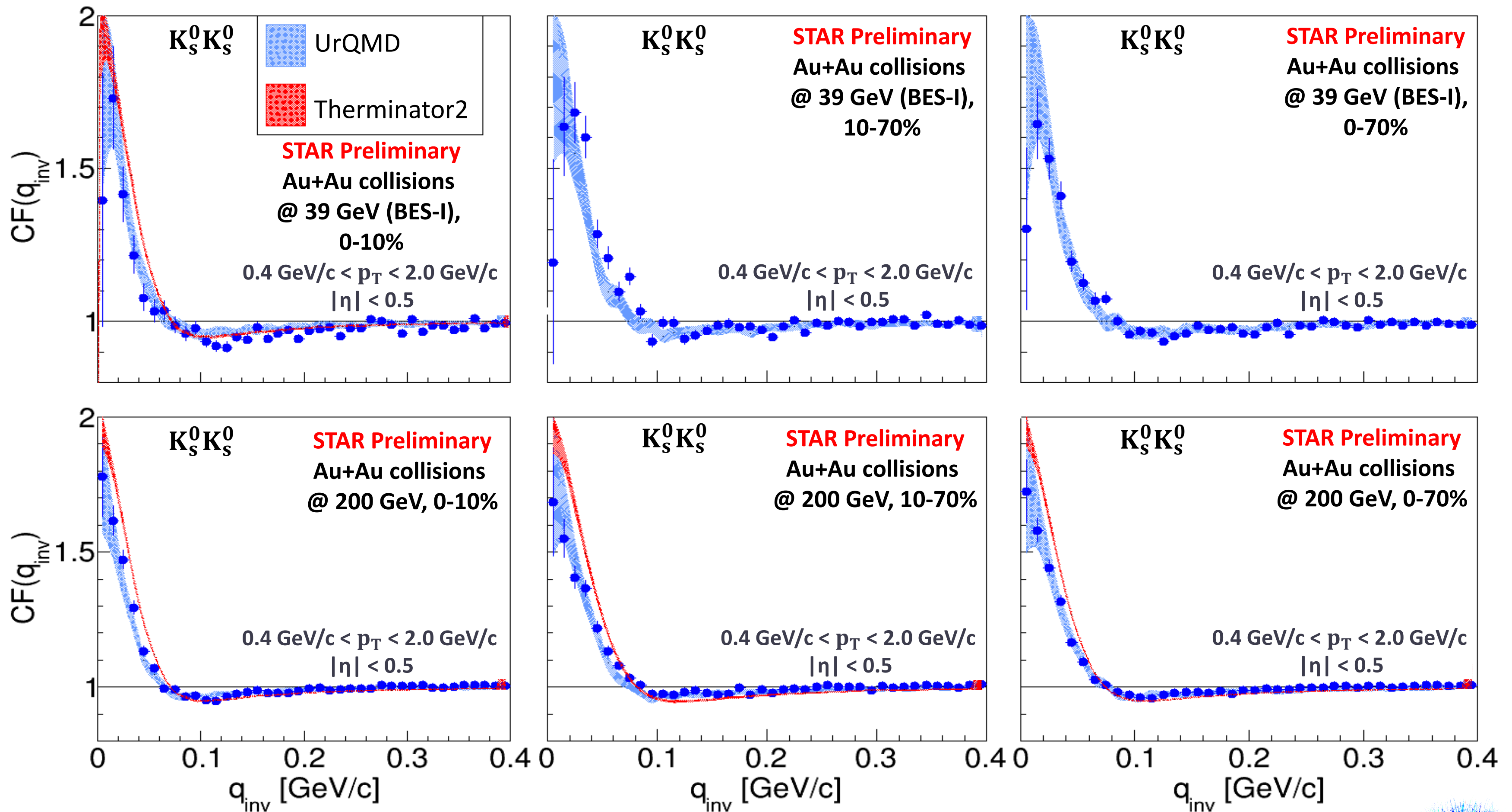
$$q_{\text{inv}} = \sqrt{(\vec{p}_1 - \vec{p}_2)^2 - (E_1 - E_2)^2}$$

$K_s^0 K_s^0$ femtoscopy at 39 GeV & 200 GeV

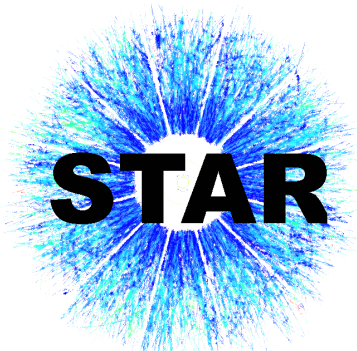


$$q_{\text{inv}} = \sqrt{(\vec{p}_1 - \vec{p}_2)^2 - (E_1 - E_2)^2}$$

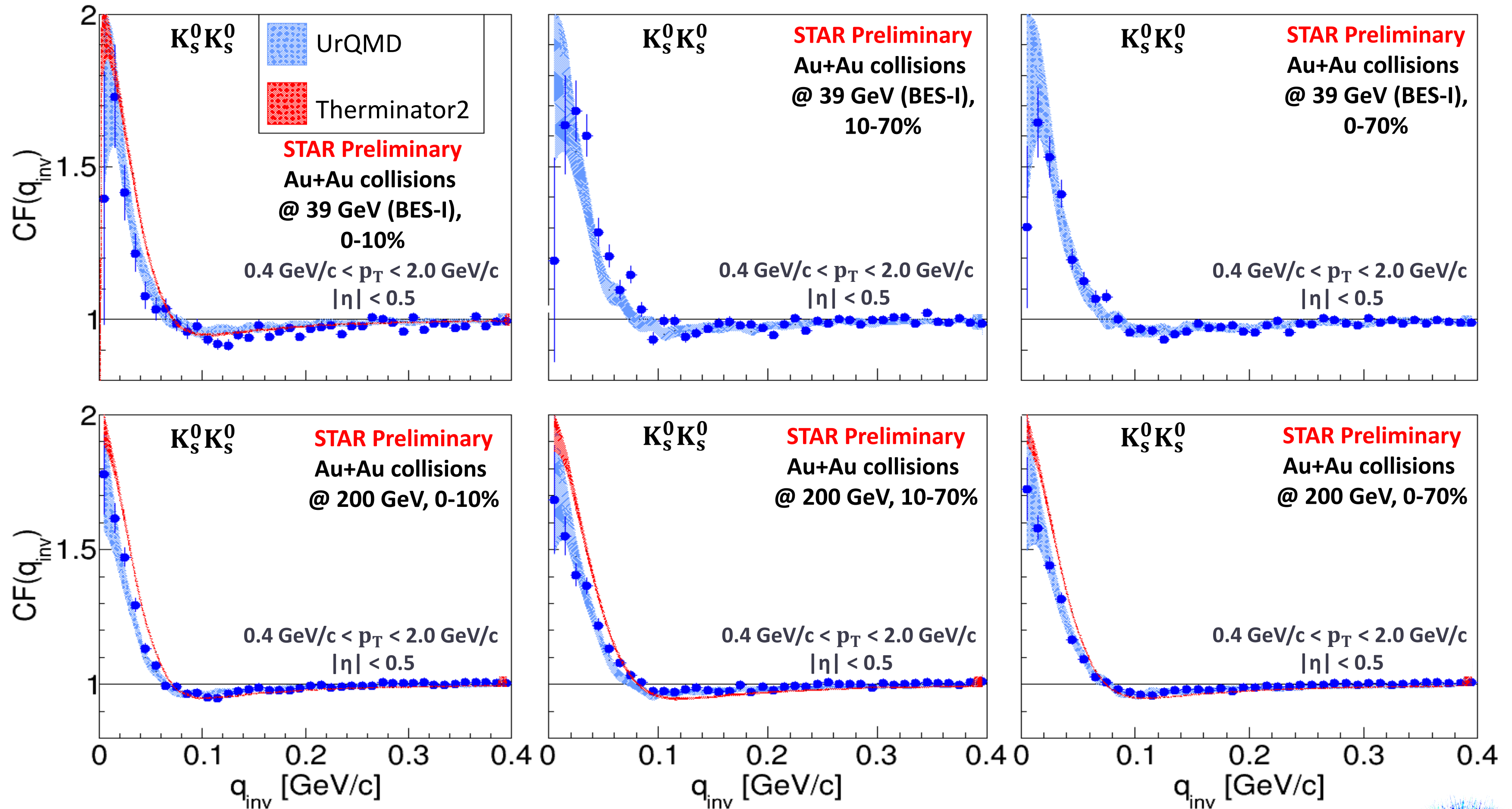
$K_s^0 K_s^0$ femtoscopy at 39 GeV & 200 GeV



$$q_{\text{inv}} = \sqrt{(\vec{p}_1 - \vec{p}_2)^2 - (E_1 - E_2)^2}$$



$K_S^0 K_S^0$ femtoscopy at 39 GeV & 200 GeV

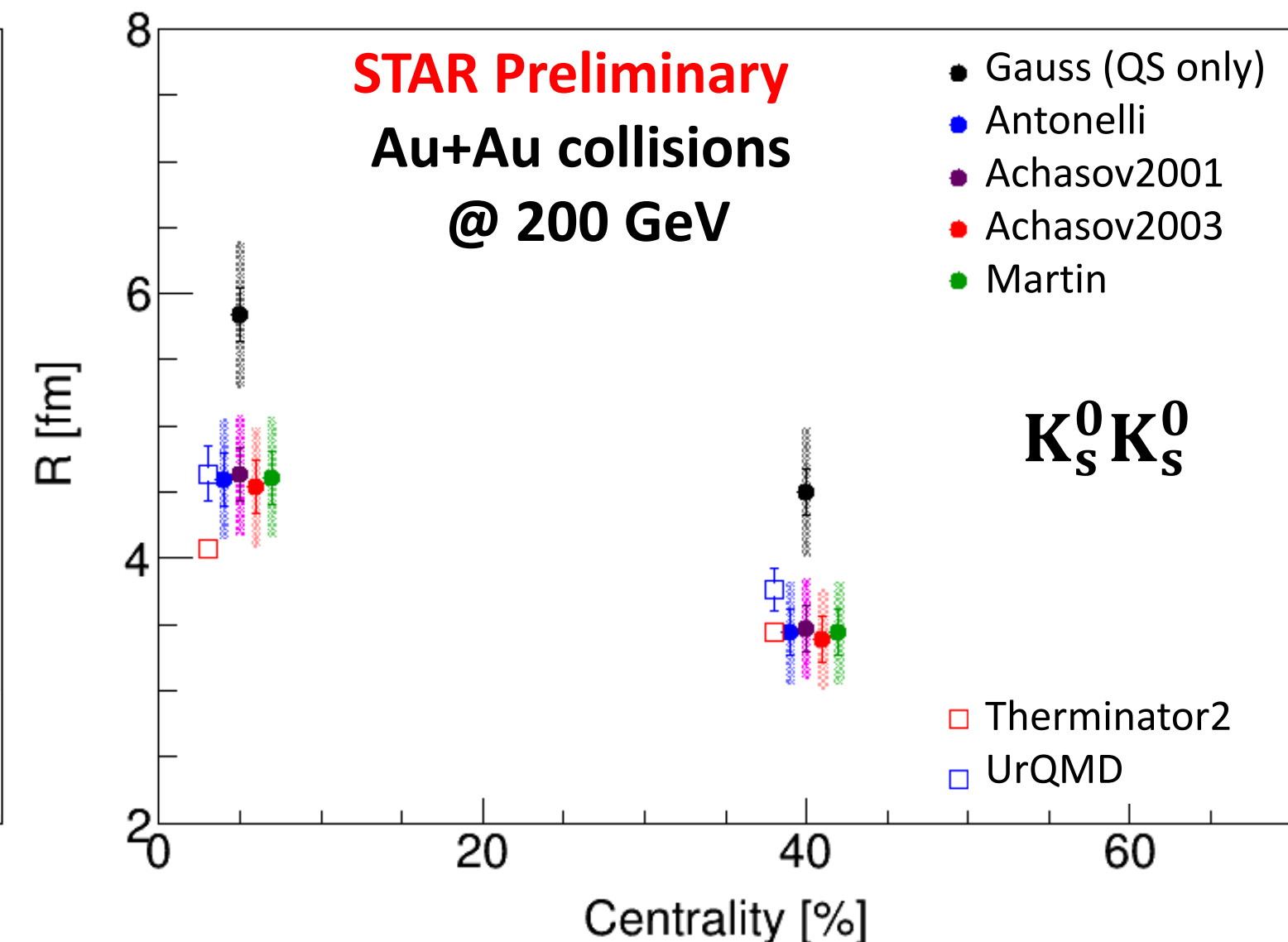
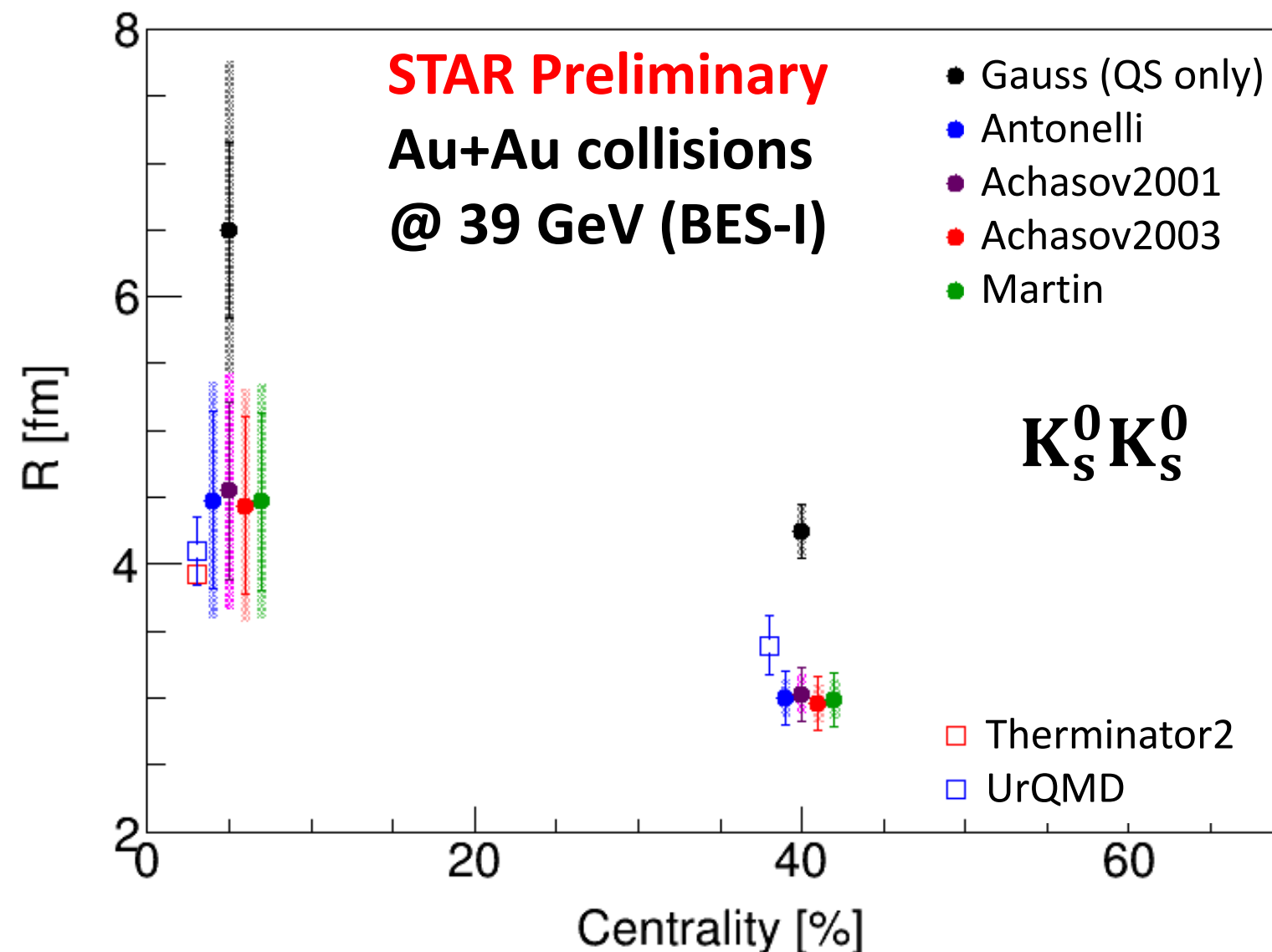


Good agreement of the experimental
points with the models

$$q_{\text{inv}} = \sqrt{(\vec{p}_1 - \vec{p}_2)^2 - (E_1 - E_2)^2}$$



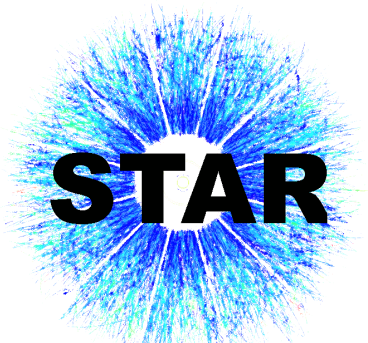
$K_s^0 K_s^0$ femtoscopy – centrality dependence



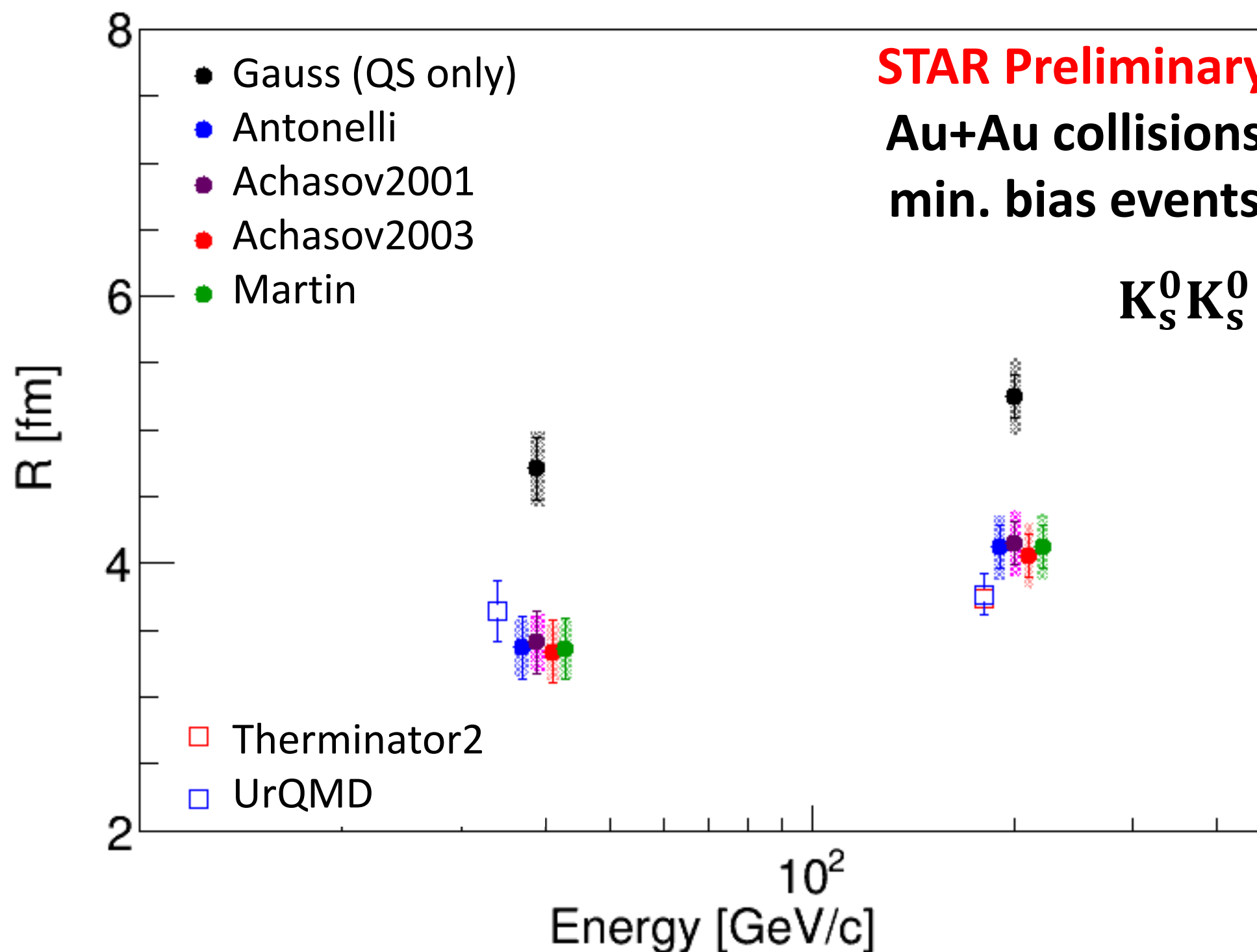
- Visible centrality dependence

$$R_{0-10\%} > R_{10-70\%}$$

- Only Gaussian assumption leads to larger R , showing importance to include SI



$K_S^0 K_S^0$ femtoscopy – energy dependence



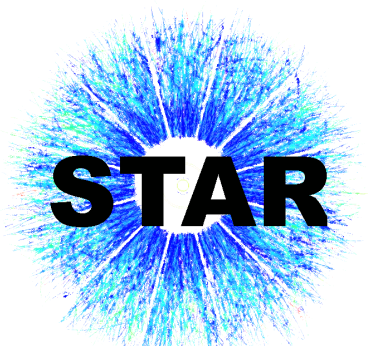
- Visible energy dependence for both parametrization $R_{200 \text{ GeV}} > R_{39 \text{ GeV}}$
- Source sizes from models and FSI parametrizations consistent within the range of uncertainty



Parametrization - $K_s^0 K^\pm$

Lednicky & Lyuboshitz model includes strong FSI: [Sov.J.Nucl.Phys. 35, 770 (1982)]

$$CF(k^*) = 1 + \frac{\lambda}{4} \left[\left| \frac{f(k^*)}{R} \right|^2 + \frac{4\Re f(k^*)}{\sqrt{\pi}R} F_1(2k^*R) - \frac{2\Im f(k^*)}{\sqrt{\pi}R} F_2(2k^*R) \right]$$



Parametrization - $K_s^0 K^\pm$

Lednicky & Lyuboshitz model includes strong FSI: [Sov.J.Nucl.Phys. 35, 770 (1982)]

$$CF(k^*) = 1 + \frac{\lambda}{4} \left[\left| \frac{f(k^*)}{R} \right|^2 + \frac{4\Re f(k^*)}{\sqrt{\pi}R} F_1(2k^*R) - \frac{2\Im f(k^*)}{\sqrt{\pi}R} F_2(2k^*R) \right]$$

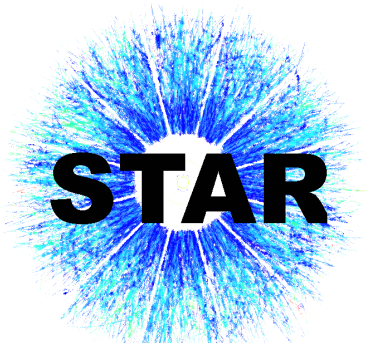
strong FSI through the $a_0(980)$ resonance

$$F_1(z) = \int_0^z dx \frac{e^{x^2} - x^2}{z}, \quad F_2(z) = \frac{1 - e^{x^2}}{z}$$

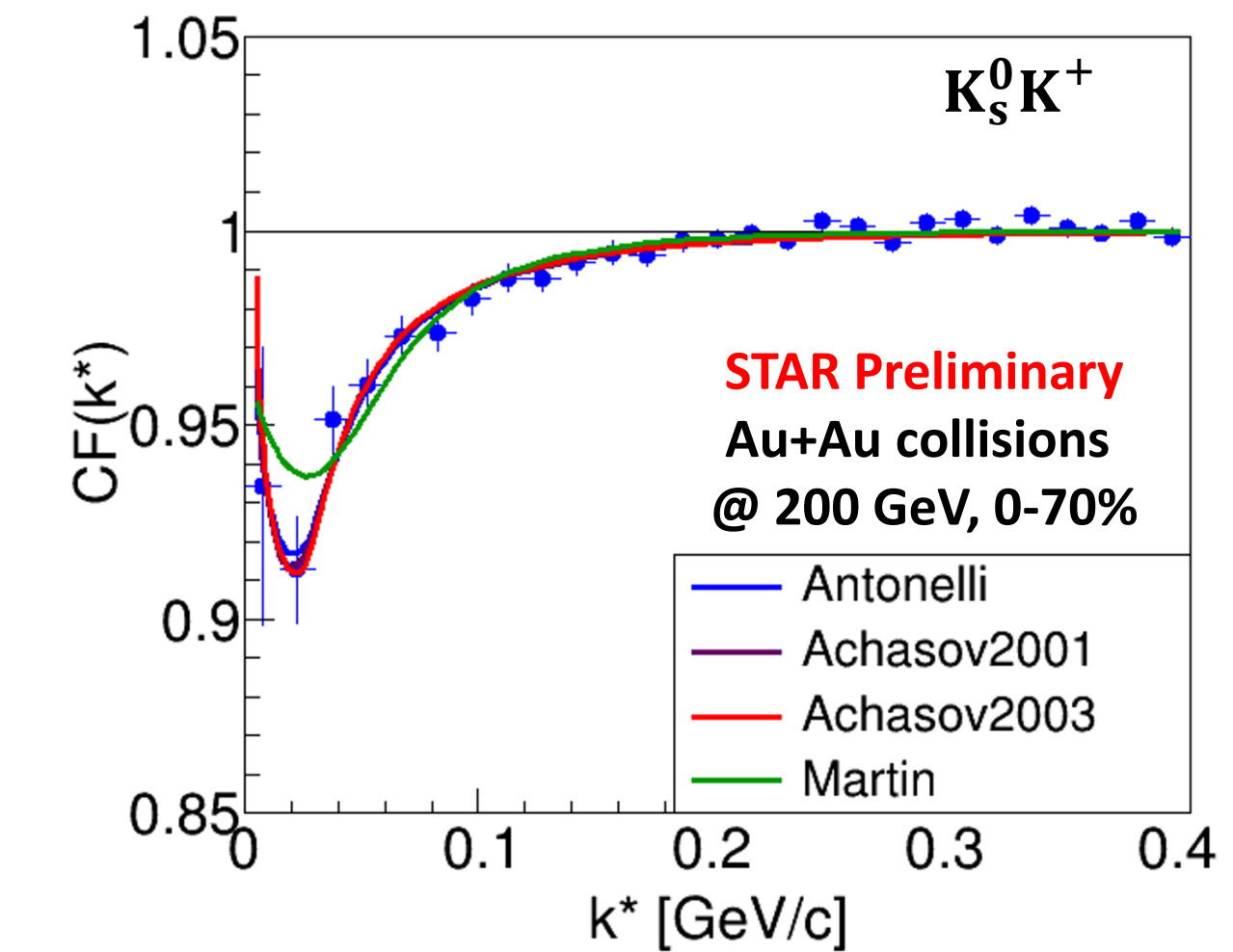
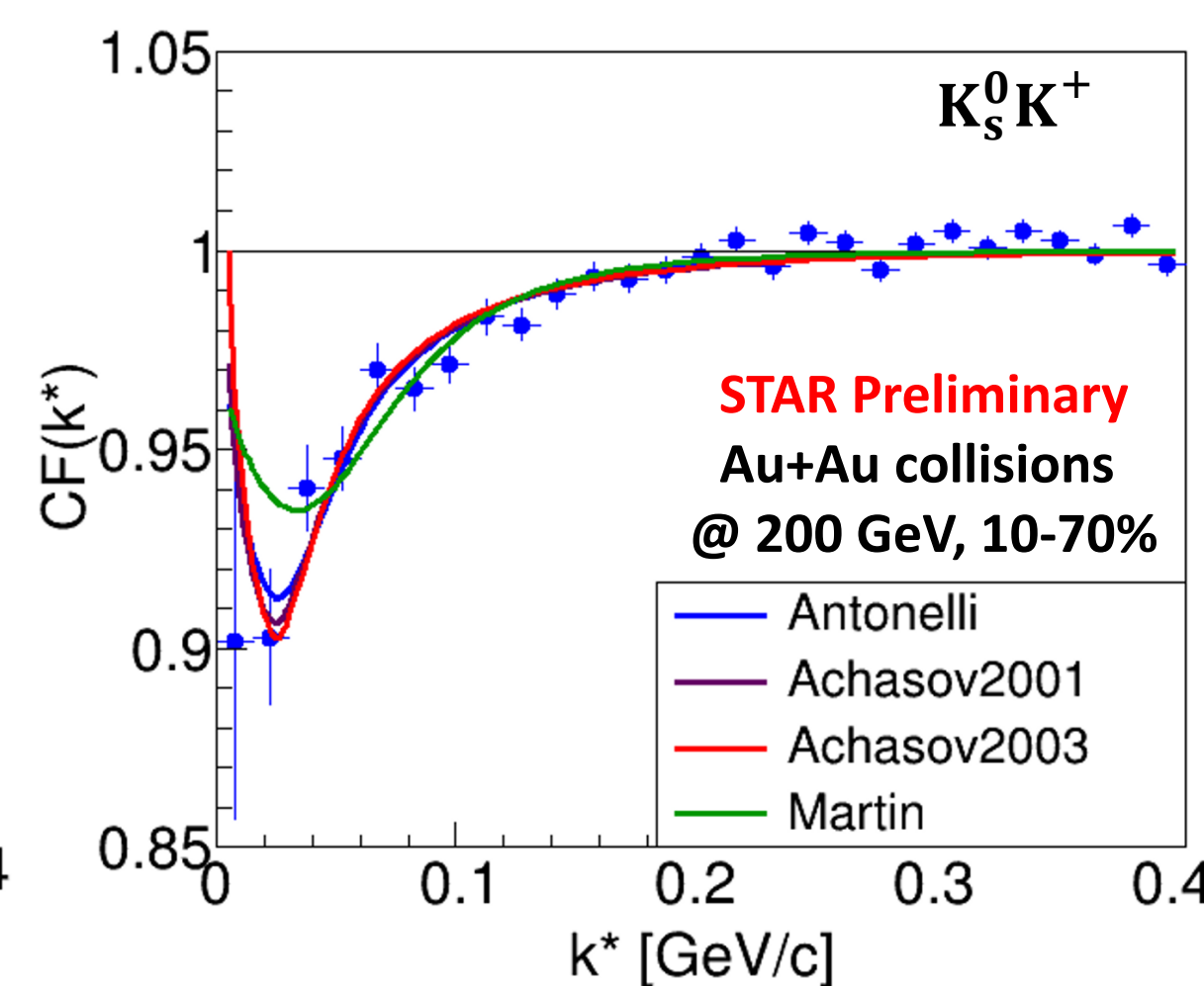
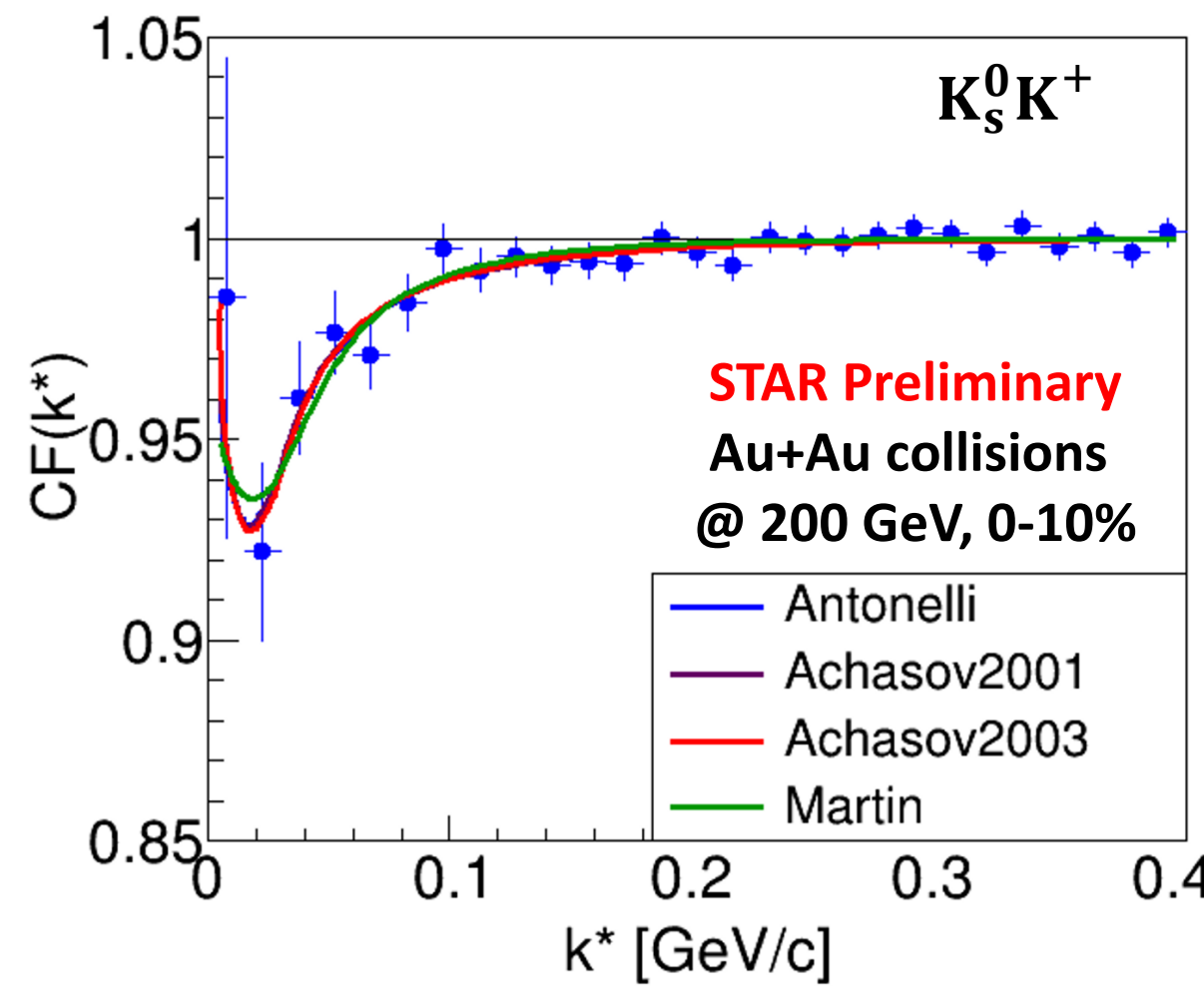
$$f(k^*) = \frac{\gamma_r}{m_r - s - i\gamma_r k^* - i\gamma'_r k'_r}, \quad s = 4(m_K^2 + k^{*2})$$

	$m_{a_0} \left[\frac{GeV}{c^2} \right]$	$\gamma_{a_0 K\bar{K}}$	$\gamma_{a_0 \pi\eta}$
Antonelli [1]	0.985	0.4038	0.3711
Achasov2001 [2]	0.992	0.5555	0.4401
Achasov2003 [3]	1.003	0.8365	0.4580
Martin [4]	0.974	0.3330	0.2220

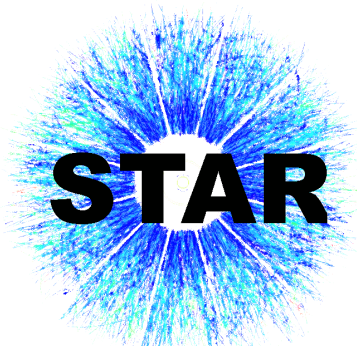
- [1] eConf C020620, THAT06 (2002), [2] Phys. Rev. D 63, 094007 (2001)
 [3] Phys. Rev. D 68, 014006 (2003), [4] Nucl. Phys. B 121, 514–530 (1977)



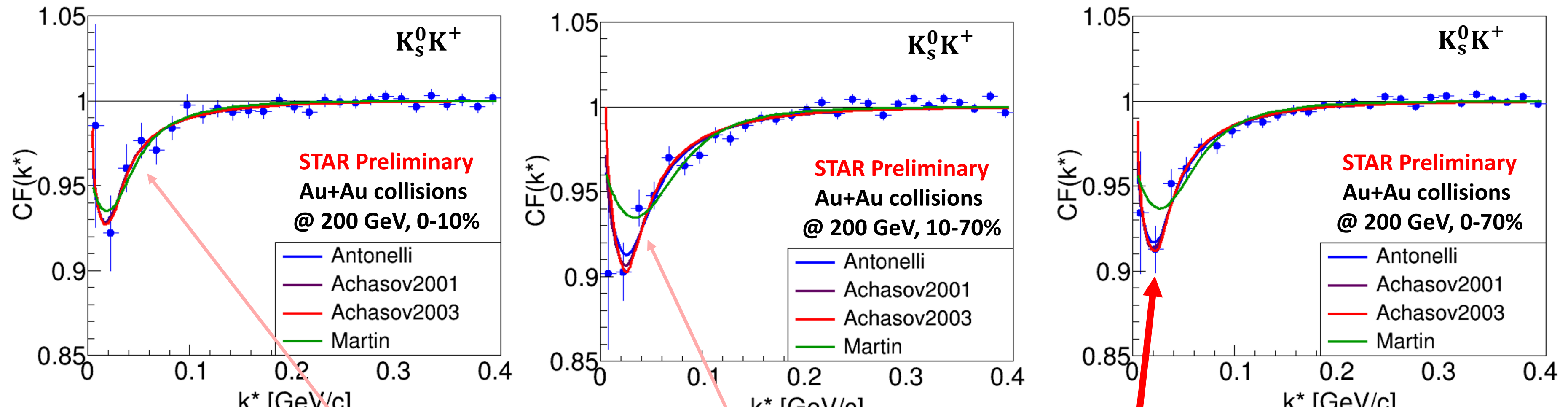
$K_s^0 K^+$ femtoscopy at 200 GeV



$$k^* = |\vec{p}_1| = |\vec{p}_2|$$



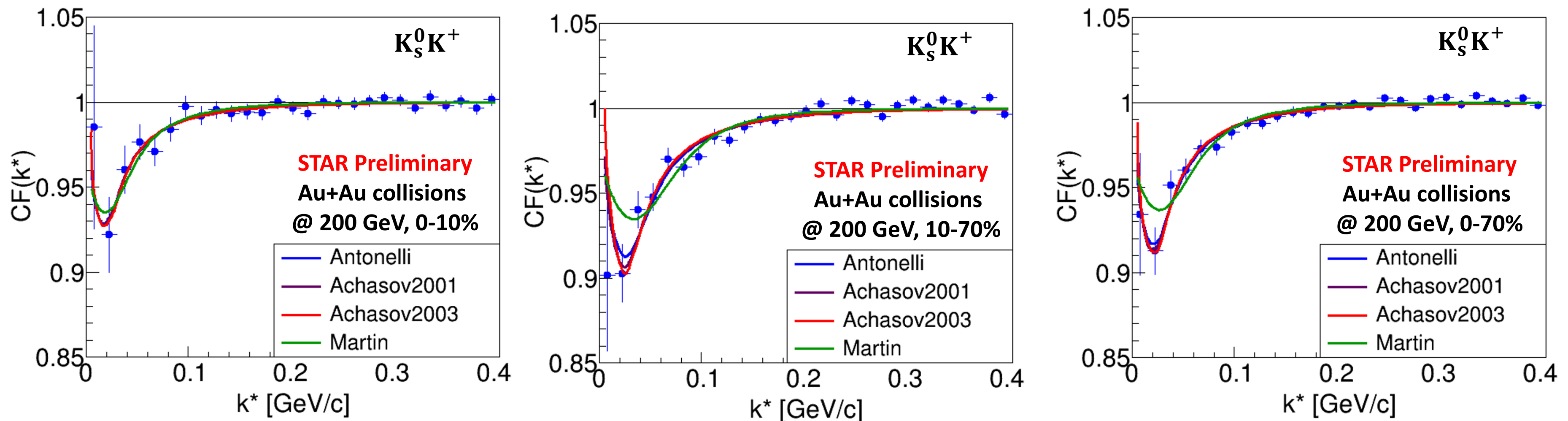
$K_s^0 K^+$ femtoscopy at 200 GeV



The α_0 FSI parametrization gives an excellent representation of the signal region of the data

$$k^* = |\vec{p}_1| = |\vec{p}_2|$$

$K_s^0 K^+$ femtoscopy at 200 GeV

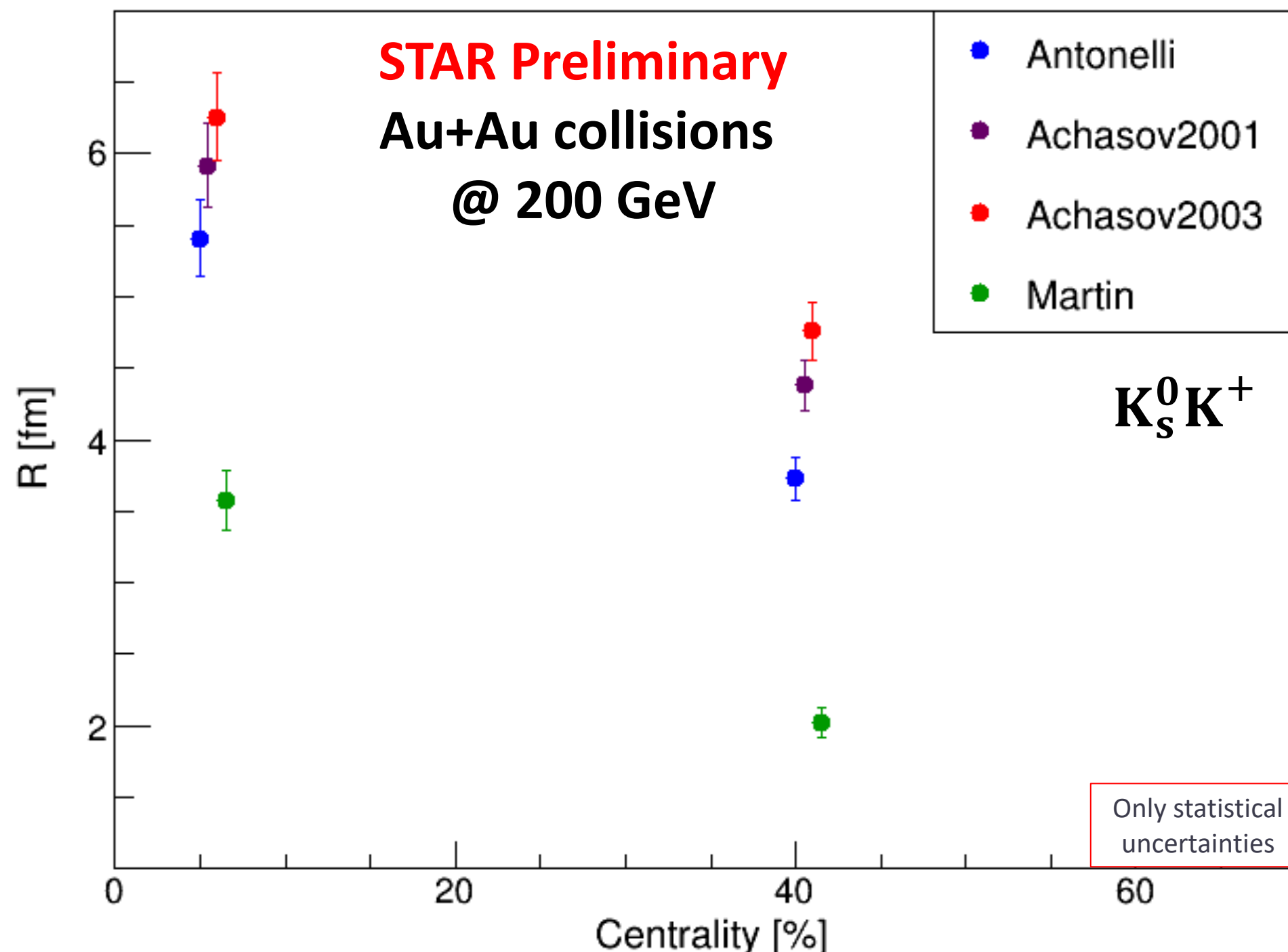

 χ^2/NDF

	0-10%	10-70%	0-70%
Antonelli [1]	0.60	1.66	1.04
Achasov2001 [2]	0.59	1.73	1.07
Achasov2003 [3]	0.58	1.85	1.14
Martin [4]	0.65	1.65	1.16

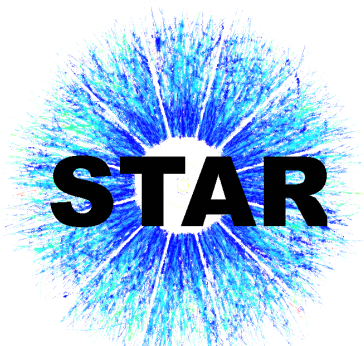
$$k^* = |\vec{p}_1| = |\vec{p}_2|$$



$K_S^0 K^+$ femtoscopy – centrality dependence

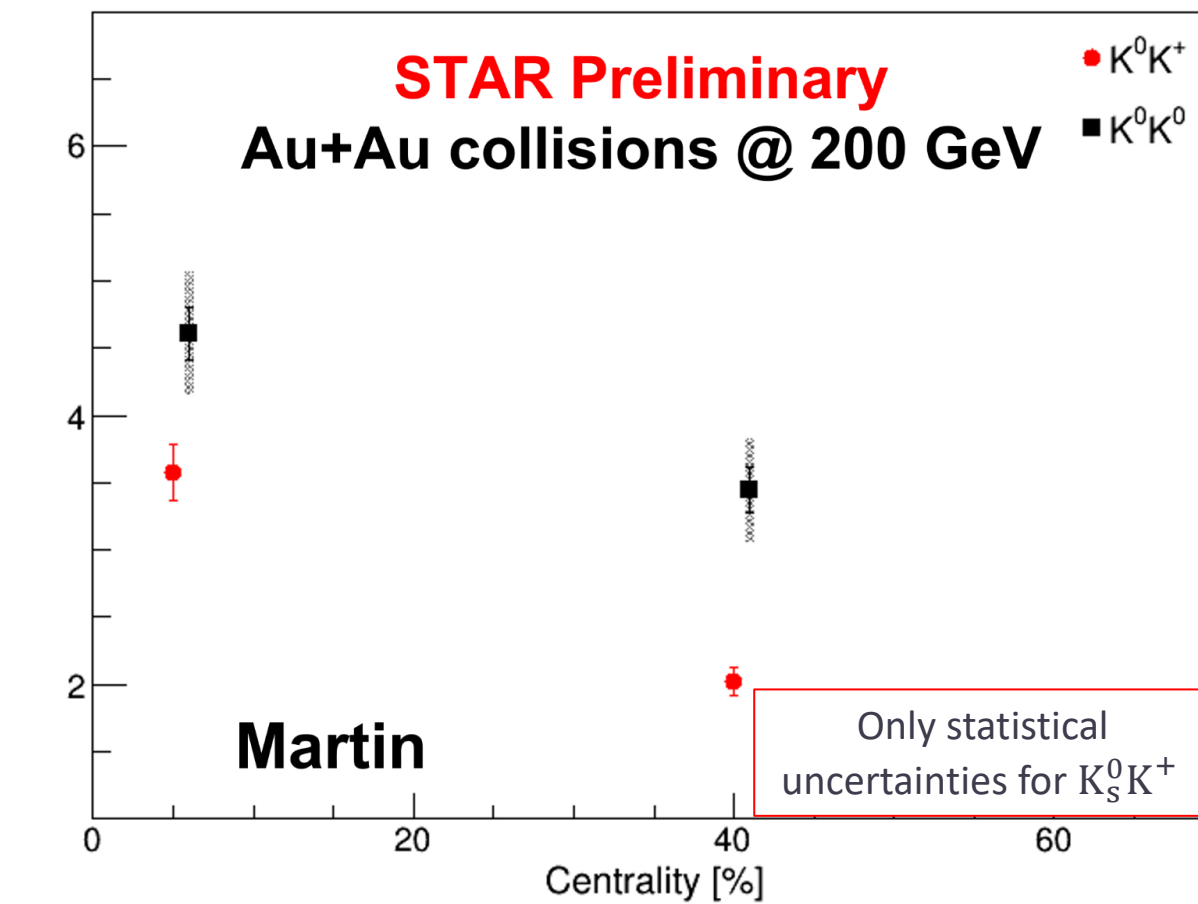
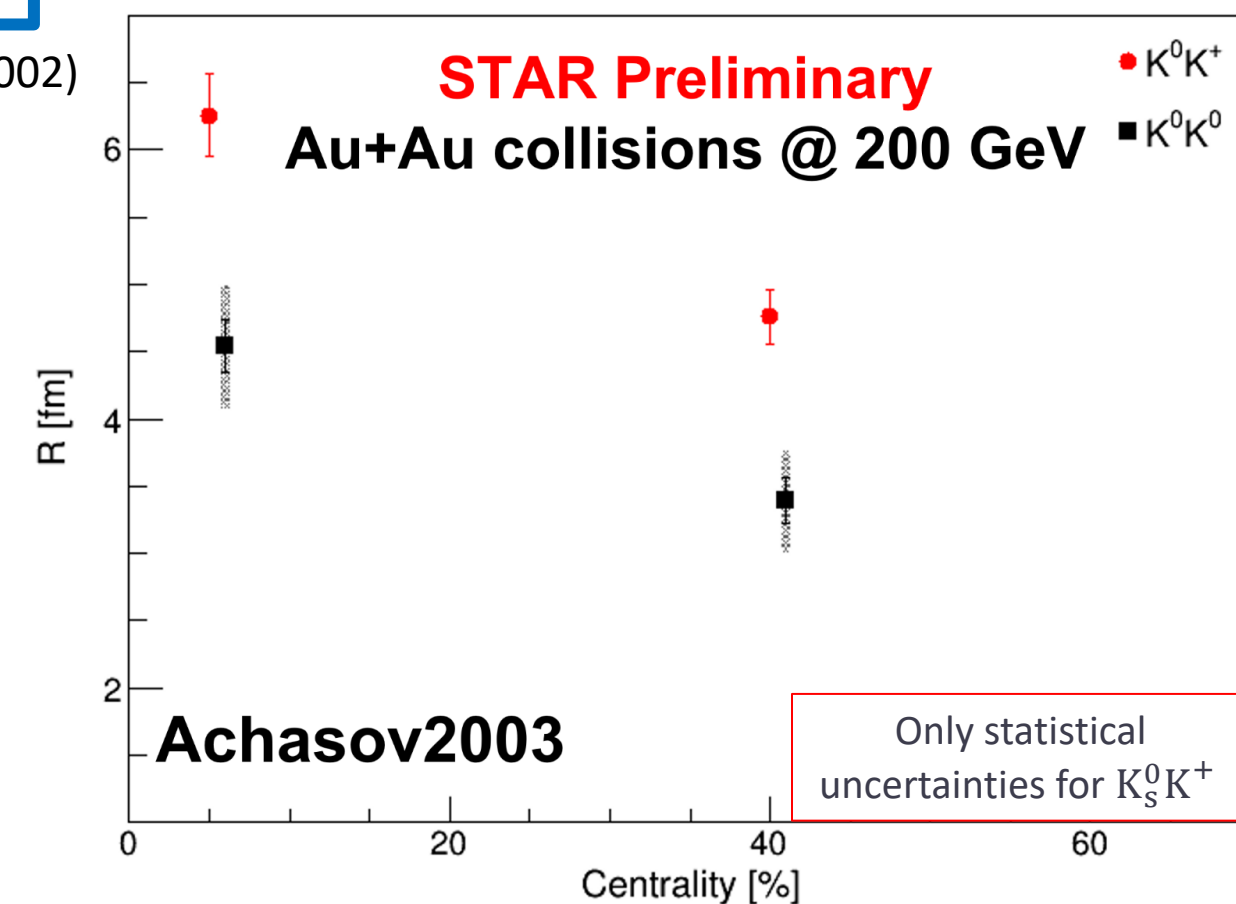
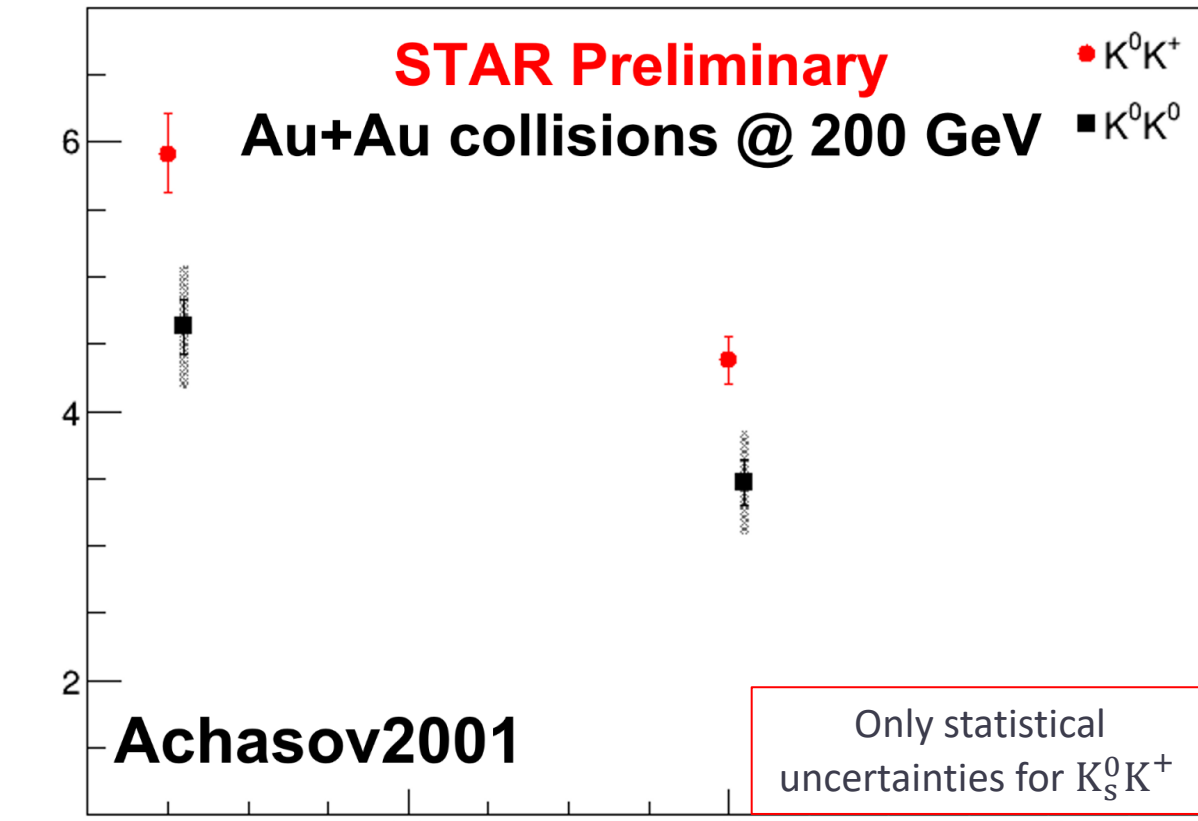
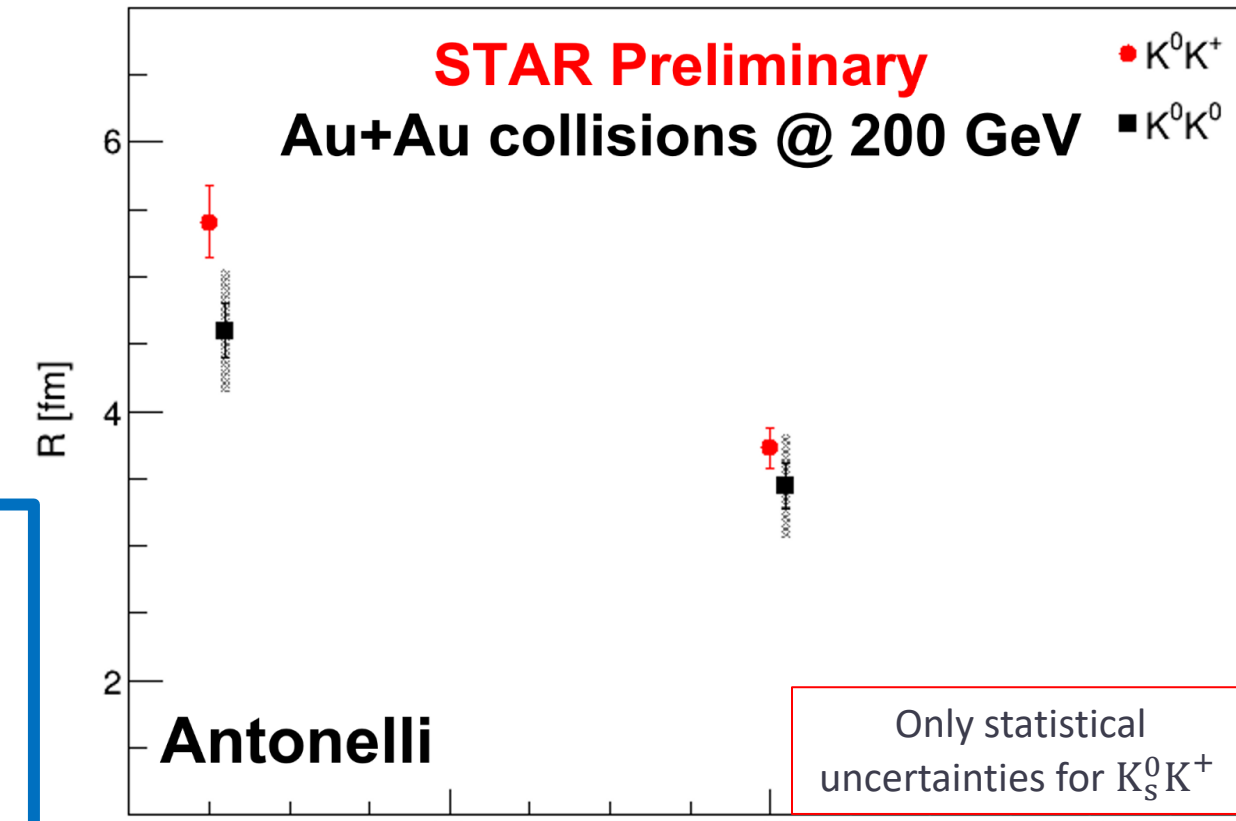


- Visible centrality dependence
 $R_{0-10\%} > R_{10-70\%}$
- Achasov2003** parametrization (the larger a_0 mass) gives the larger size of the source



Comparison - $K_S^0 K_S^0$ and $K_S^0 K^+$ - 200 GeV

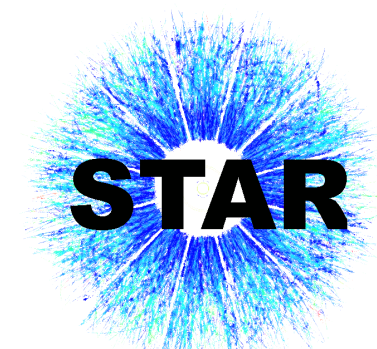
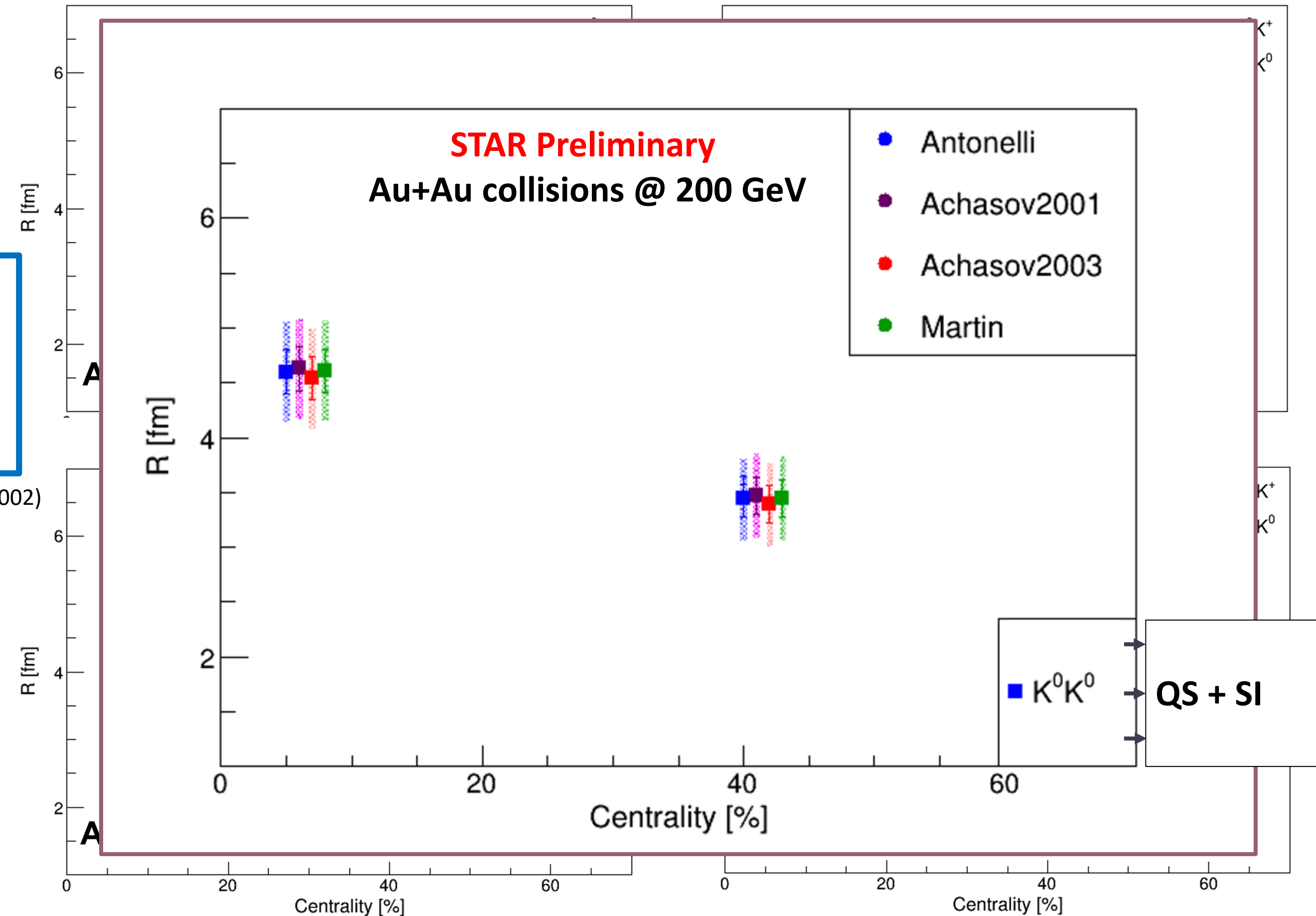
Antonelli
favors a_0
resonance as
a tetraquark



Comparison - $K_S^0 K_S^0$ and $K_S^0 K^+$ - 200 GeV

Antonelli
favors a_0
resonance as
a tetraquark

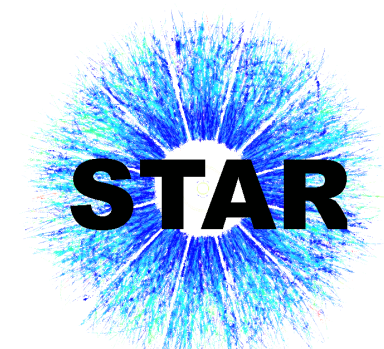
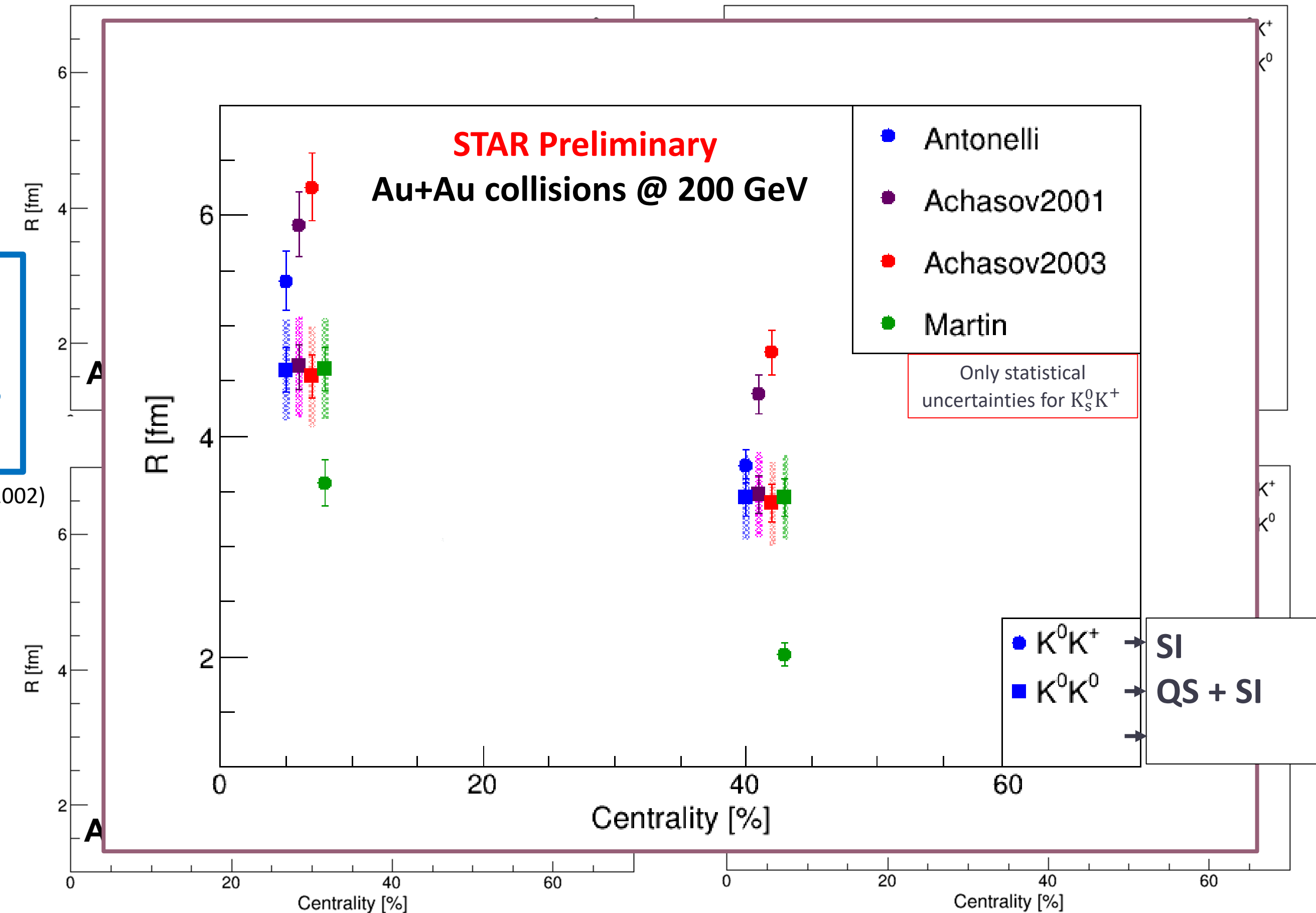
eConf C020620, THAT06 (2002)



Comparison - $K_S^0 K_S^0$ and $K_S^0 K^+$ - 200 GeV

Antonelli
favors a_0
resonance as
a tetraquark

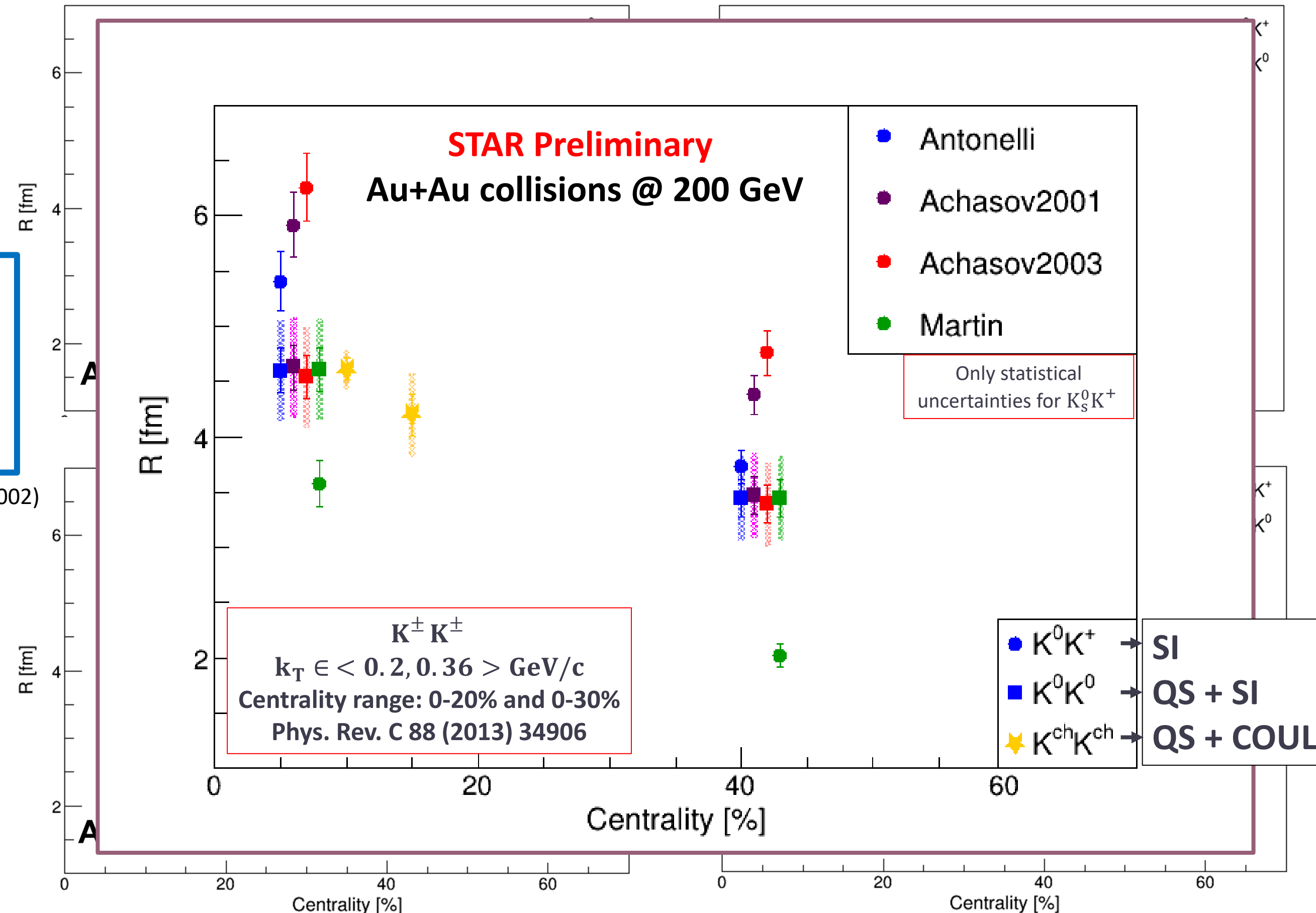
eConf C020620, THAT06 (2002)



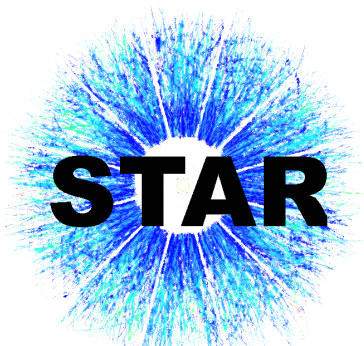
Comparison - $K_S^0 K_S^0$ and $K_S^0 K^+$ - 200 GeV

Antonelli
favors a_0
resonance as
a tetraquark

eConf C020620, THAT06 (2002)



$$R_{K^\pm K^\pm} = \sqrt{\frac{R_{out}^2 + R_{side}^2 + R_{long}^2}{3}}$$



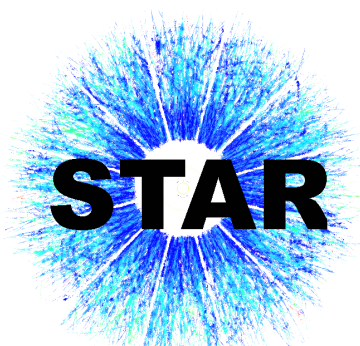
Summary

$K_s^0 K_s^0$ femtoscopy

- The strong final-state interaction has a significant effect on the $K_s^0 K_s^0$ correlation due to the near-threshold $f_0(980)$ and $a_0(980)$ resonances
- The radii of the source depend on centrality and increase with increasing collision energy
- Extracted source radii are comparable to these from models

$K_s^0 K^+$ femtoscopy

- The $a_0(980)$ FSI parametrization gives very good representation of the shape of the signal region in CF
- The parametrization with the larger $a_0(980)$ mass and decay coupling gives larger size of the source
- Comparison with $K_s^0 K_s^0$
 - Antonelli parametrization favors $a_0(980)$ resonance as a tetraquark



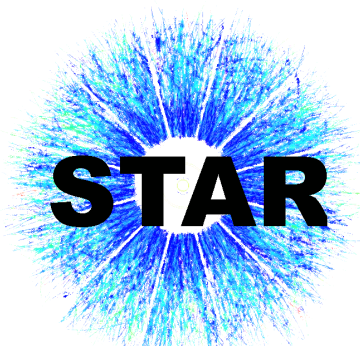
Summary

$K_s^0 K_s^0$ femtoscopy

- The strong final-state interaction has a significant effect on the $K_s^0 K_s^0$ correlation due to the near-threshold $f_0(980)$ and $a_0(980)$ resonances
- The radii of the source depend on centrality and increase with increasing collision energy
- Extracted source radii are comparable to these from models

$K_s^0 K^+$ femtoscopy

- The $a_0(980)$ FSI parametrization gives very good representation of the shape of the signal region in CF
- The parametrization with the larger $a_0(980)$ mass and decay coupling gives larger size of the source
- Comparison with $K_s^0 K_s^0$
 - Antonelli parametrization favors $a_0(980)$ resonance as a tetraquark



Summary

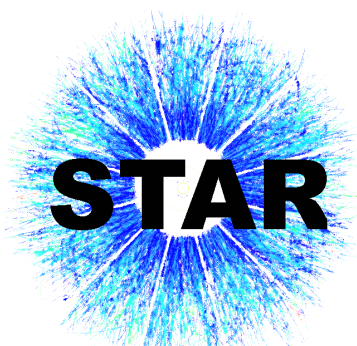
$K_s^0 K_s^0$ femtoscopy

- The strong final-state interaction has a significant effect on the $K_s^0 K_s^0$ correlation due to the near-threshold $f_0(980)$ and $a_0(980)$ resonances
- The radii of the source depend on centrality and increase with increasing collision energy
- Extracted source radii are comparable to these from models

$K_s^0 K^+$ femtoscopy

- The $a_0(980)$ FSI parametrization gives very good representation of the shape of the signal region in CF
- The parametrization with the larger $a_0(980)$ mass and decay coupling gives larger size of the source
- Comparison with $K_s^0 K_s^0$
 - Antonelli parametrization favors $a_0(980)$ resonance as a tetraquark

Compatibility of source sizes for $K_s^0 K_s^0$, $K_s^0 K^+$ and $K^\pm K^\pm$ pairs in the case of Antonelli



Summary

$K_s^0 K_s^0$ femtoscopy

- The strong final-state interaction has a significant effect on the $K_s^0 K_s^0$ correlation due to the near-threshold $f_0(980)$ and $a_0(980)$ resonances
- The radius of the source increases with energy
- Extract $K_s^0 K^+$ femtoscopy
- The $a_0(980)$ shape changes
- The parameterization gives larger size of the source
- Comparison with $K_s^0 K_s^0$
 - Antonelli parametrization favors $a_0(980)$ resonance as a tetraquark

Outlook

**High statistic BES-II data give the ability
to analyze neutral kaon femtoscopy for
energies $\sqrt{s_{NN}} < 20 \text{ GeV}$**

Compatibility of source sizes for $K_s^0 K_s^0$, $K_s^0 K^+$
and $K^\pm K^\pm$ pairs in the case of Antonelli



Thank you for your attention!!

